



# Investigating the Palaeoshorelines and Coastal Archaeology of the Southern Red Sea

Robyn H. Inglis, William Bosworth, Najeeb M. A. Rasul, Ali O. Al-Saeedi, and Geoff N. Bailey

## Abstract

Numerous palaeoshoreline features including coral platforms, beachrock and wave-cut notches are present on the Red Sea coastline of SW Saudi Arabia and on the Farasan Islands. Some are associated with prehistoric archaeological material, which has been the focus of ongoing archaeological investigations over the past decade. Dating and interpretation of these features are therefore of considerable interest and relevance to the deep history of human coastal adaptation and colonization in a key zone for the understanding of early human expansion out of Africa, as well as to the study of relative sea-level changes and tectonic movements. This chapter provides details of a field survey carried out in 2014 and presents new information on the location, geological setting, geochronological sampling and archaeological associations of these palaeoshoreline features. The results of dating are still awaited, so that some of our interpretations are still hypotheses in need of further testing. At this stage, it is clear that the most prominent shoreline features on the mainland coast are at elevations similar to those

dated elsewhere in the Red Sea as belonging to MIS 5e, and that in at least one exposure Middle Stone Age artefacts can be stratigraphically linked with this period of high sea level. On the Farasan Islands, coral platforms have undergone more variable and localised rates of movement associated with salt tectonics. We set out the field data in support of these interpretations and consider their wider archaeological and tectonic implications.

## 1 Introduction

The purpose of this chapter is to present the results of a field excursion conducted in November and December 2014 to examine palaeoshoreline features in the southern Red Sea along the mainland coastline of Asir Province in SW Saudi Arabia and on the Farasan Islands in Jizan Province (Fig. 1), and to set out the intellectual and scientific issues that have informed our fieldwork.

Cemented coral platforms and beach deposits indicating the presence of palaeoshorelines are widely distributed above present sea level around the Red Sea, and some have been recorded below sea level (Faure et al. 1980; Dullo 1990; Hoang and Taviani 1991; El Moursi et al. 1994; Gvirtzman 1994; Hoang et al. 1996; Plaziat et al. 1998, 2008; Walter et al. 2000; Lambeck et al. 2011; Manaa et al. 2016; Bosworth et al., this volume; Sakellariou et al., this volume). Those on land mostly represent earlier periods of high sea level during Pleistocene interglacials. They occur at varying elevations above present sea level, up to 100 m in the Gulf of Aqaba, reflecting differences of age, variations in eustatic sea level in different interglacials, and vertical crustal movements associated with tectonic processes of various sorts.

Similar palaeoshoreline features are present in our region. In particular, exposures of cemented coral platforms or terraces and beach deposits at least 4 m above the present sea level, and assumed to relate to higher sea-level stands of the

R. H. Inglis (✉) · G. N. Bailey  
Department of Archaeology, University of York, The King's  
Manor, YO1 7EP York, UK  
e-mail: robyn.inglis@york.ac.uk

R. H. Inglis  
Department of Environmental Sciences, Macquarie University,  
North Ryde, Sydney, NSW 2109, Australia

W. Bosworth  
Apache Egypt Companies, 11 Street 281, New Maadi, Cairo,  
Egypt

N. M. A. Rasul  
Center for Marine Geology, Saudi Geological Survey, Jeddah,  
Saudi Arabia

A. O. Al-Saeedi  
Survey Department, Saudi Geological Survey, Jeddah, Saudi  
Arabia

G. N. Bailey  
College of Humanities, Arts and Social Sciences, Flinders  
University, GPO Box 2100 5001 Adelaide, SA, Australia

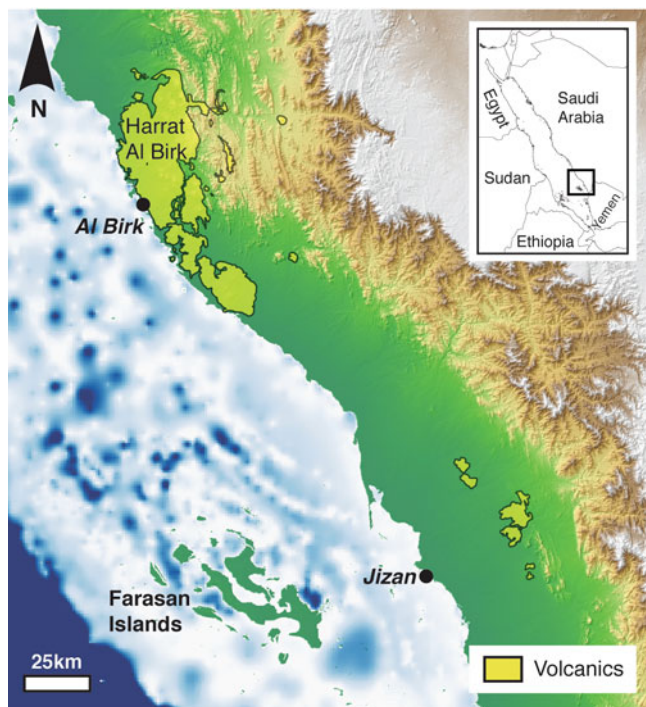


**Fig. 1** The southwestern Saudi Arabian Red Sea coastline showing the Harrat al Birk and Farasan Islands. Area of Fig. 4 outlined in black. Pale blue areas show the continental shelf exposed when sea level is lowered to 120 m. The dark blue circular patches on the shelf are deep depressions resulting from solution of Miocene evaporites. Data from GEBCO 08 and SRTM 4.1

Last Interglacial period (MIS 5e) or older, have been noted during earlier archaeological expeditions in the region (Zarins et al. 1980, 1981; Alsharekh and Bailey 2013; Bailey et al. 2007a, b; Inglis et al. 2013, 2014a, b). However, they had not received systematic or extensive geological investigation or geochronological sampling before our 2014 expedition. As such, the region is one of the least well studied in this respect compared to most other coastlines of the Red Sea. It is also the focus of ongoing research on coastal prehistory (Bailey et al. 2012, 2015; Devès et al. 2013; Inglis et al. 2013, 2014a, b, 2015; Meredith-Williams et al. 2013, 2014; Bailey and Alsharekh, in press; Bailey et al., this volume; Hausmann et al., this volume; Sinclair et al., this volume), and this provides an additional incentive for more detailed geological research. Moreover, many coastal features are under threat of destruction by intensifying pressures of development, road-building, other infrastructural projects and tourism, adding urgency to the collection of field data.

For most published studies, the primary interest of these palaeoshoreline features is their contribution to an understanding of sea-level change, and that is often taken to be the main goal of their investigation. Together with evidence from deep sea cores (Siddall et al. 2003; Rohling et al.

2013), this makes the Red Sea an important study region for the wider understanding of global sea level change and its relationship to climate change. However, palaeoshoreline features also have relevance to a wider range of geological, geoarchaeological and archaeological interests, and it is important to be clear about the different aims, data requirements and assumptions that different disciplines bring to shoreline studies. We identify here broadly three different themes:

1. Measurement and modelling of sea-level change in relation to global climate change, often with the ultimate goal of producing better predictions of future sea-level change.
2. Understanding of regional tectonic effects associated with rifting, plate motions and other processes of crustal deformation and their contribution to the wider understanding of Earth deformation processes and geodynamics
3. Charting the role of coastlines in the global expansion of human populations out of Africa during the Pleistocene period and the deeper history of human interest in coastal and marine resources and their exploitation.

These three themes are, of course, interlinked. Shoreline features cannot be interpreted as sea-level indicators without taking into account the interplay between eustatic variations of sea level and vertical crustal movements associated with rifting, plate motions, changes of mass loading and other tectonic effects. This is especially important in the Red Sea, which has a complex geotectonic history. Palaeoshorelines in their turn provide sensitive measures of tectonic movements that can be calibrated against independent evidence of eustatic sea level change. Eustatic changes of sea level also have effects on the mass loading of the Earth's crust in coastal regions and on the erosion or submergence of geological features. In relation to archaeological issues, both tectonic and sea-level changes alter the physical landscape setting within which past human populations made their living; they can alter the nature and accessibility of the plants, animals and water supplies available for subsistence, pathways of movement and communication, and the preservation and visibility of archaeological evidence. Geological studies can also provide chronological control on the archaeology. Geologists and sea-level specialists in their turn are interested in the potential of archaeological data to provide independent age-constraints on geological processes, and are increasingly interested in the relevance of their research to the study of human evolution and the scale of human activities (e.g., Lambeck et al. 2011; Rohling et al. 2013; Benjamin et al. 2017; Kübler et al., this volume).

Shoreline features are viewed differently in each of these types of investigation—as sea-level indicators, as measures of tectonic movement, and as evidence of human exploitation of shorelines, respectively. The measurement accuracy differs accordingly. For sea-level studies, measurements of the highest possible accuracy are required—metre to decimetre scale—with clear specification of measurement errors and other sources of uncertainty, and calibration to a uniform spatial and temporal framework. This is to facilitate differentiation of eustatic sea levels in different interglacials or interglacial sub-stages that may differ by only a small amount, and to facilitate interregional and global comparisons. For tectonic studies, a coarser scale—metres to tens of metres—may be sufficient to distinguish between stable conditions and long-term vertical movements. For archaeological purposes, the absolute height of a shoreline is less important than stratigraphic evidence that the archaeological material can be directly associated with an elevated shoreline feature at the time when sea level was high, rather than representing material deposited on the surface at a later date. For example, stone tools found on the surface of Last Interglacial coral terraces could have been deposited during the subsequent glacial stage, when sea level was far lower than present and the shoreline many tens of kilometres distant.

Despite these inter-relationships and the widely acknowledged virtues of interdisciplinary research, the investigation of these three themes is often pursued by scientific communities working within separate disciplinary or subdisciplinary compartments with poor communication across the boundaries between them or even mutual incomprehension. As a multi-disciplinary group with combined expertise in geoarchaeology, marine science, coastal prehistory, geophysics and tectonic geology, we are interested in all three of these themes and the relationships between them, and our approach to field surveying has been shaped accordingly.

In this chapter, we set out the wider geological and archaeological issues that inform our fieldwork, define our field objectives and methods, present our preliminary results, and discuss their wider implications.

---

## 2 Geological and Archaeological Issues

### 2.1 Geological Context

The Red Sea has a geotectonic setting involving the interaction of several different processes, including: continental rifting involving crustal extension, normal faulting and volcanism; seafloor spreading; plate motions; isostatic changes of mass loading; and more localised tectonic movements resulting from the mobility of Miocene salt deposits, also referred to as evaporites or halites. The basin began to take its present form as a continental rift at about

30 Ma as a northward extension of the East African Rift system, and this whole rift structure was probably triggered at least in part by the eruption of the 4 km-thick flood basalts that occurred over the Ethiopian hot spot—a swelling and thinning of the Earth's crust over a hot plume rising from deep within the Earth's mantle—acting on pre-existing weaknesses in the lithosphere (Hubert-Ferrari et al. 2003; Bonatti et al. 2015; Bosworth 2015). The central Red Sea basin has the typical features and asymmetric cross-section of a rift, with the main faulting running through the centre of the basin. Ongoing extension and normal faulting have resulted in progressive uplift of the rift flanks and deepening of the rift floor. The footwall of the main rift is on the eastern margin, comprising the western Arabian escarpment, which reaches a maximum height of ~3000 m above sea level (asl) in the south; the lower, hanging wall is on the western margin of the Red Sea; and the deepest part of the axial trough in the centre of the basin is ~2800 m below present sea level.

By 19 Ma, seafloor spreading had commenced in the Gulf of Aden. The Arabian Peninsula continued separating from the African Plate, moving to the north, with extension in the Afar region of Ethiopia and the widening of the 'Proto Red Sea'. The Red Sea remained isolated from the world oceans, apart from intermittent incursions of seawater from the Mediterranean, and filled with thick deposits of evaporite because of high rates of evaporation in a closed basin. By 5 Ma, a connection with the Indian Ocean was established, with the onset of seafloor spreading and formation of oceanic crust within the Red Sea Basin. The whole process has been accompanied by episodes of magmatism on land on the Arabian side with extensive areas of volcanic cinder cones and basaltic lava flows, notably during the Miocene (>5 Ma) and the Quaternary (<2 Ma and extending in some regions into the Holocene), although it remains unclear to what extent these originate from shallow sources in the mantle associated with local extension and faulting or from deeper mantle sources associated with the Ethiopian plume.

Many of the details of these processes including their timing and the nature of ongoing deformation are still a matter for debate. An active oceanic spreading centre is present along the basin axis, with the Arabian Plate separating from Africa/Nubia at ~1.7 cm/yr (ArRajehi et al. 2010), and continuing to slide along the large transform faults that define its western and eastern boundaries and to collide with the Eurasian continent to the north. However, there is debate concerning when the transition from continental rifting to seafloor spreading began (Girdler and Styles 1974; Girdler and Whitmarsh 1974; Cochran 1983; Coleman 1993; Cochran and Karner 2007; Mohriak 2015). Plate reconstructions and extrapolation of spreading rates suggest that the tectonic regime has been fairly constant over about the past 11 Myr (McQuarrie et al. 2003; Reilinger et al. 2015).

Despite considerable understanding of the nature of the plate boundary running through the centre of the southern Red Sea, there remain fundamental questions about both the long- and short-term response of the continental margins to this relatively young oceanic rifting. There is no question that the uplifted margins of the southern Red Sea rift underwent a significant period of uplift and denudation during the Early Miocene after the commencement of continental rifting (Bohannon 1986; Bohannon et al. 1989; McGuire and Bohannon 1989; Bosworth and Stockli 2016). However, it remains unclear whether uplift is still occurring and, if so, to what extent it is the result of faulting and extension associated with rifting and ocean spreading or of thermal expansion linked to the Ethiopian plume. The stark relief of the Arabian Escarpment, with peaks of over 3000 m (Spohner and Oelman 1986; Coleman 1993) might suggest ongoing uplift. Data discussed below indicate that some parts of the coastline appear to have been stable during the Late Pleistocene. However, such data need to be interpreted in the light of models of isostatic adjustment (Lambeck et al. 2011). In other regions, the localized effects of plate motions have resulted in significant vertical movement (tens of metres within the Quaternary period), particularly in the north along the Dead Sea transform fault (the Sinai Peninsula and Gulf of Aqaba). Other areas have been subjected to local instability with faulting and uplift resulting from the movement of deposits of Miocene evaporite, notably the Farasan Islands (Bosence et al. 1998; Dullo and Montagnoni 1998).

Providing new constraints on the evidence for vertical movements of the southern Arabian margin will help address these important issues. Better understanding of these tectonic processes also has obvious relevance in correcting the derivation of sea-level position from palaeoshoreline features, and in addition it has an important role to play in the interpretation of archaeological evidence for the early human colonization and occupation of the Arabian Peninsula.

## 2.2 Archaeological Context

The coastal regions of the Red Sea Basin play a key role in understanding the global dispersal of human populations from Africa during the Pleistocene (Bailey et al. 2007a, b). At least two major episodes of dispersal are recognised, the first of *Homo erectus* or *H. ergaster*, at about 1.8 Ma, using a Lower Palaeolithic/Early Stone Age (ESA) technology, and a later dispersal of *H. sapiens* populations with Middle Palaeolithic/Middle Stone Age (MSA) technology at some time between 190 ka (the earliest dated appearance of anatomically modern *H. sapiens* in Africa) and 60 ka (the arrival of *H. sapiens* in Australia). It has generally been assumed that the main pathway of expansion was via the

Nile-Sinai land route in the north, but there is growing interest in the possibility that human populations were able to cross at the southern end in the vicinity of the Hanish Sill and the Bab al Mandab during periods of low sea level. This idea has found particular favour in discussion of *H. sapiens* dispersal, along with the hypothesis that their ability to make sea crossings was facilitated by new adaptations in the exploitation of marine resources and the use of simple sea craft, but use of the southern route by earlier populations cannot be excluded (Beyin 2006; Bailey 2009, 2015; Lambeck et al. 2011; Mellars et al. 2013; Erlandson and Braje 2015). Certainly, the sea channel in the south would have been very narrow for long periods of the Pleistocene and the coastal landscapes on the Arabian side would have benefited from the orographic rainfall attracted by the highest parts of the Arabian Escarpment. These relatively humid conditions would have provided attractive environments for human occupation during all climatic phases of the Pleistocene compared to the more arid interior (Bailey et al. 2015).

These contrasting opinions have recently crystallised into a debate between two contrasting models of population expansion for *H. sapiens* (Groucutt et al. 2015; Petraglia et al., this volume). One, the ‘Late Dispersal/Coastal Highway’ model, draws on phylogenetic trees constructed from similarities in the mitochondrial DNA of modern populations in Asia and Africa, and on comparisons between the South African and South Asian archaeological records, to propose a rapid dispersal of populations adapted to marine resources and coastal environments around the Indian Ocean rim at 60–50 ka (Macaulay et al. 2005; Mellars et al. 2013). The second, the ‘Early Dispersal/Green Arabia’ model, highlights ambiguities in the DNA evidence and emphasises the evidence for the extension of grasslands and lakes into the interior of the Arabian Peninsula during a wetter climatic interval in early MIS 5 and the presence of MSA archaeological sites in lake edge settings dating to the same time interval at about 130–120 ka (Parker 2009; Armitage et al. 2011; Petraglia et al. 2011, this volume; Rose et al. 2011; Rosenberg et al. 2013). Of course, these models are not mutually exclusive and both earlier and later dispersals are possible using both interior and coastal pathways of expansion.

The major difficulty with the coastal model is the extreme rarity or absence of archaeological sites in coastal locations. For the Late Dispersal Model, this may be explained by the fact that sea levels were substantially lower at 60 ka and the relevant shorelines and sites are hidden underwater or destroyed. However, even on coastlines with steeply shelving offshore bathymetry and on Last Interglacial shorelines exposed above modern sea level, such sites are very rare, the notable exception being Abdur on the Eritrean shore of the Red Sea dated at 130 ka (Walter et al. 2000).

Absence of evidence is not decisive, and may reflect lack of discovery or a variety of taphonomic factors at the coast

edge affecting the visibility and preservation of archaeological material (see Bailey et al., this volume). Evidence of Pleistocene coastal activity is very rare everywhere, and the best-known examples occur in sediments accumulated in coastal caves in South Africa and on various coastlines of the Mediterranean and Atlantic Europe, where the cave setting provides a protective environment for the preservation and easy discovery of dateable and stratified sediments with archaeological evidence (Erlandson 2001; Bailey et al. 2008; Jerardino 2017). In any case, these debates place a high premium on the search for Pleistocene archaeological sites in coastal settings, and beach deposits of Last Interglacial date (MIS 5e) are a prime target for investigation.

Coral terraces associated with earlier periods of high sea level of Last Interglacial date or earlier are especially prominent in the Harrat Al Birk region of the Asir Province, where they are found along many parts of the coastline in close association with an extensive outcrop of Pleistocene volcanic cones and lava fields (Dabbagh et al. 1984), and on the Farasan Islands, where they are a dominant land form and have clearly been subjected to differential warping and uplift by salt doming (McFadyen 1930). In both regions, archaeological material is associated with these coral terraces. In the Harrat Al Birk, MSA stone tools made on basaltic lava are located on the surface of many coral terraces as well as in locations further inland (Fig. 2; see also Sinclair et al., this volume). Major issues here are the chrono-stratigraphic links between the archaeology, the coral terraces and the basaltic lava flows, and more specifically the question of whether the stone tools can be stratigraphically or chronologically linked to the period of high sea level when the corals were forming.

On the Farasan Islands, some 3000 mid-Holocene shell middens radiocarbon-dated between 6.5–4.5 ka, including substantial mounds easily visible on satellite imagery, are located on the edge of coral platforms along the modern coastline. In places, these platforms are elevated some 2–3 m above the present sea level and have been undercut by marine erosion to form a well-defined notch (Fig. 3; Bailey et al. 2013a, this volume; Meredith-Williams et al. 2013, 2014; Alsharekh and Bailey 2013; Bailey and Alsharekh 2018). These are all cultural deposits where mollusc shells have accumulated as food debris. Some are shell scatters, while others have formed impressive mounds as much as 5 m thick resulting from repeated use of the same place over many decades or centuries for the processing of shellfood. Rare stone tools are associated with these shell deposits, including ones made from volcanic stone brought from the mainland, very rare potsherds, hearths, fish bones and occasional bones of gazelle. The cultural material and non-molluscan food remains are sparse, reflecting both the



**Fig. 2** Examples of Palaeolithic artefacts from the Harrat al Birk collected during January 2015 fieldwork: 1 Potential prepared core (MSA); 2 Small exhausted discoidal core (potentially MSA); 3 Cleaver (ESA); 4 Large flake/scrapper (ESA). Photos: Frederick Foulds and Andy Shuttleworth, January 2015



**Fig. 3** Shell mound in Janaba Bay, Farasan al Kabir, Farasan Islands. The shell mound sits on the edge of a coral platform, and the notch formed by marine erosion is clearly visible beneath the mound. Photo: Geoff Bailey, December 2014

rapid accumulation and large volume of deposits composed mostly of shell debris, and the rarity of suitable raw material on the islands for making stone artefacts. Seasonality studies of the shells show that they were eaten during all periods of the year (Hausmann and Meredith-Williams 2017), but the vast quantities of discarded shells almost certainly

over-represent the contribution of the molluscs as food, and other resources, particularly fish, were undoubtedly important.

In both regions, the archaeology provides a minimum age for the underlying coral platforms, but the gap in time between the archaeology and the formation of the underlying surface may be very large. Hence, the archaeology cannot be relied on to provide an age constraint on the geology, except at best a minimum date. For example, the coral platform on which the Farasan shell mounds are located is thought to be of Last Interglacial date even though the shell mounds are clearly mid-Holocene in age; MSA stone tools were in use over many tens of thousands or even hundreds of thousands of years. Dating of geological formations is more likely to help the archaeological interpretation rather than the reverse, but in all cases the question of stratigraphic association between geological deposits and archaeological material is critical to understanding the past use of coastal landscapes

### 3 Field Objectives and Methods

#### 3.1 Field Objectives

Field objectives were as follows, to:

- Study the structural geology of coastal land forms and associated evidence of faulting, fracturing and volcanism.
- Locate fossil marine and beach deposits that represent earlier periods of high sea level.
- Measure the elevation of these deposits in order to track local and regional changes in the Earth's crust resulting from rifting and salt tectonics, and to provide new data on sea-level change.
- Collect samples for dating by Uranium-series (U-series), Amino Acid Racemization (AAR) or Argon-Argon ( $^{40}\text{Ar}/^{39}\text{Ar}$ ) dating according to local circumstances.
- Relate the geological history of these coastal areas to the archaeological sites which are frequently found at the coast edge in association with marine deposits.

#### 3.2 Definitions and Field Methods

Coral and marine terraces in the Harrat al Birk and the Farasan Islands were surveyed over seven days in November–December 2014. Sites for investigation were selected through examination of satellite imagery (e.g., Google Earth, Landsat GeoCover Mosaics) and knowledge of locations derived from previous field surveys by ourselves and others (Dabbagh et al. 1984; Bantan 1999; Inglis et al. 2014b). Locations visited were traversed by 4-wheel drive vehicles and on foot. Within

the Farasan archipelago a small motorboat was also used to access the coastlines of several islands.

#### 3.3 Palaeoshoreline Feature Description and Sampling

In this paper, we use the term 'beachrock' to refer to a lithified coastal deposit consisting of beach sediments that have become cemented through carbonate precipitation on the immediate shoreline (following Mauz et al. 2015). 'Coral terrace' refers to extant deposits of fossil coral that consist primarily of coral skeletons in growth position, with varying amounts of broken coral. Other types of marine deposits are discussed where relevant.

Most of the coral and beach deposits we examined are heavily cemented, and particular attention was devoted to the collection of samples of coral for U-series dating. The degraded nature of the coral material necessitated an intensive search for suitable in situ specimens that had undergone the least alteration. Moreover, the heavily cemented nature of the deposits required heavy-duty hammers and chisels and prolonged effort to extract suitable samples. Most of the coral we examined is unsuitable for dating because of its fibrous open structure and risk of diagenetic alteration and contamination. Many coral samples when broken open showed streaks of mineral staining, a sign of probable contamination. The most suitable material for dating is large coral heads with a dense and uniform structure, and we preferentially selected corals of this type occurring in growth position and containing little detritus or obvious diagenetic alteration. Weathered material was removed mechanically from the samples in laboratories at the Center for Marine Geology at the Saudi Geological Survey in Jeddah, and these were then sent to the Research School of Earth Sciences at the Australian National University for U-series dating.

Shells of large gastropods and the *Tridacna* clam were also collected and submitted to the Department of Chemistry, University of York, for AAR dating. Shell material of this type, as well as coral, is potentially amenable to AAR dating, and can provide reliable age estimates and measures of post-depositional alteration that can aid in assessing the results of U-series dating (Penkman et al. 2008; Hendy et al. 2012).

Basalt samples were removed from key exposures for  $^{40}\text{Ar}/^{39}\text{Ar}$  dating to constrain the geological history and stratigraphic relationships of marine deposits and have been submitted to the USGS in Denver, USA. OSL dating of marine and aeolian sands at Dhahaban Quarry is also underway at the Scottish Universities Environmental Research Centre, East Kilbride (Sanderson and Kinnaird, this volume).

### 3.4 Feature Measurement and Correction to Elevation Above Mean Sea Level

The heights and locations of the surfaces of beachrock and coral terraces, and of dating samples collected from them, were recorded using a Trimble DGPS. We used the same equipment to make additional traverses and spot elevations of specific features, and to geo-reference the base stations of a fuller total station survey undertaken earlier in 2014 at Dhahaban Quarry (Inglis et al. 2014a). Each locality is designated by a sequential number and the date (e.g., '2014-12-05-5' is the fifth station surveyed on December 5, 2014). In some locations additional elevation data were also obtained by tape measure to sea level. In the Harrat al Birk region, all of these localities had been previously, or were subsequently, surveyed for archaeological artefacts, by the UK-Saudi DISPERSE project and assigned locality numbers (e.g., L0103), numbers that are also referenced here to aid cross-referencing between publications (Inglis et al. 2013, 2014b, 2015; Sinclair et al., this volume).

Each DGPS base station was set up using the sea-level on the nearest beach as the local datum, with the measurements from each station later adjusted to their position above mean sea level through reference to local tide data. According to Bruckner et al. (2011), the annual tidal range in the Red Sea today varies along its length, being highest in the north and the south (2.0 m and 1.4 m respectively), and lowest in the middle (0.5 m), but these are clearly general averages. The nearest sources of tidal data for Al Birk and the Farasan Islands are Al Qunfudah and Jizan, respectively. Here the maximum tidal range derived from daily measurements throughout 2014 is 1.76 m and 1.69 m respectively (data supplied by the General Commission for Survey of Saudi Arabia). We have used the tidal position closest to the time of our DGPS readings to measure the offset between the sea-level surface at the time of the reading and mean sea level (Table 1), and used this to correct our field measurements of palaeoshoreline features to heights above modern mean sea level. For example, a coral terrace measured in the field using Al Birk Station 2 (offset +0.58 m) at an elevation of 3.45 m on the Al Birk coastline represents an elevation of

**Table 1** Correction factors for DGPS readings taken at different stations in the study area in order to convert elevations of palaeoshoreline features to elevations above modern mean sea level. The original elevations were measured above a local datum consisting of the sea surface at the time of measurement. The correction factors have been calculated by reference to the nearest available tide tables. See the notes below the table and the text for further explanation

Station Name	Date <sup>a</sup>	Time <sup>a</sup>	Sea-Level Datum (m)	Measurement Error (m) <sup>b</sup>	Tidal Station <sup>c</sup>	Tidal Position (m) <sup>d</sup>	Tidal Error <sup>e</sup>	Annual Max Tidal Range (m)	Mean Sea Level (m) <sup>f</sup>	Correction (m) <sup>g</sup>
Sulayn	30/11/2014	11.45	0	±0.1	Jizan	0.4402	±0.02	-0.10 to +1.59	0.75	-0.31
Farasan Station 2	01/12/2014	9.20	0	±0.03	Jizan	0.566	±0.01	-0.10 to +1.59	0.75	-0.18
Farasan Station 3	01/12/2014	11.10	-1.7	±0.05	Jizan	0.9018	±0.01	-0.10 to +1.59	0.75	+1.55
Dhahaban Station	03/12/2014	13.23	0	±0.03	Qunfudah	0.6092	±0.01	-0.803 to +0.975	0.08	+0.53
Al Birk Station 1	04/12/2014	16.23	0	±0.02	Qunfudah	0.492	±0.01	-0.803 to +0.975	0.08	+0.41
Al Birk Station 2	04/12/2014	13.02	0	±0.01	Qunfudah	0.6609	±0.00	-0.803 to +0.975	0.08	+0.58
Al Birk Station 3	05/12/2014	12.51	0	±0	Qunfudah	0.659	±0.01	-0.803 to +0.975	0.08	+0.58
North of 'Amq	05/12/2014	15.04	0	±0.1	Qunfudah	0.5813	±0	-0.803 to +0.975	0.08	+0.50
Qamah	06/12/2014	09.51	0	±0.02	Qunfudah	0.5442	±0.01	-0.803 to +0.975	0.08	+0.46

<sup>a</sup>Time of sea-water surface measurement

<sup>b</sup>Range of variation in measurement of sea-water surface

<sup>c</sup>Location of nearest tidal gauge with hourly records of tidal position

<sup>d</sup>Estimate of water level to the nearest half hour based on 2014 tidal tables

<sup>e</sup>Allows for difference between estimated and actual tidal position at time of measurement

<sup>f</sup>Mid-point of the maximum annual tidal range

<sup>g</sup>Figure to be added to field elevations to give height above modern mean sea level

4.03 m above modern mean sea level. The measurements referred to throughout the text in the results section below are these measurements with the offsets applied, and are therefore metres above mean sea level (amsl).

### 3.5 Palaeo Sea-Level Estimates

Important in palaeo sea-level estimates are regional measures of the vertical relationships between shoreline features and mean sea-level position, using modern analogues and taking account of such factors as the depth over which a particular indicator is formed ('the indicative range'), tidal range and measurement errors or uncertainties (Mauz et al. 2015; Rovere et al. 2016). In order to estimate the palaeo mean sea-level position in this paper, we make three assumptions: that the tidal range was the same as the modern one; that the surface of the living coral reef approximates the low water mark (0.89 m below mean sea level on the Al Birk coastline); and that the surface of beachrock approximates high water mark (0.89 above mean sea level at Al Birk). In both cases, for ease of reference and in recognition of the difficulties with establishing precise constraints, we round these figures to 1 m.

This gives an offset of +1 m for estimating palaeo mean-sea-level from coral terraces, and -1 m when using elevations of beachrock. Thus, we assign a coral terrace measured at an elevation of 4.03 m amsl on the Al Birk coastline an estimated palaeo mean-sea-level of 5.03 m above modern mean sea level. Similarly, a beachrock elevation of 6.85 m amsl gives an estimated palaeo mean sea level of 5.85 m.

These palaeo sea-level corrections may be too large given that beach deposits may form at different levels across a beach profile in relation to tidal range (Mauz et al. 2015), and that there is some variation in the depth relationship between mean sea level and the surface of the living coral, depending amongst other factors on whether it is a reef flat, a reef crest or a fore reef. We do not have detailed measurements or geomorphic descriptions of beach profiles or living coral reefs in our region to provide suitable analogues. We therefore rely on data from the published literature; in the Red Sea, the living coral surface is usually taken to approximate the low water mark (Lambeck et al. 2011; Manaa et al. 2016). Lambeck et al. (2011) cite figures for the height of mean sea-level above the coral reef surface as +0.5 to +1.0 m and use +0.5 m while Manaa et al. (2016) use an average of +0.3 m based on local measurements of the modern coral surface and the local tidal range. For beach deposits, Lambeck et al. (2011) cite a variety of figures indicating heights of +1.5 to +2.5 m above the coral surface. Our figures differ from those used by Lambeck et al (2011) and Manaa et al. (2016), although not substantially, and we

attribute these differences to differences in tidal range (or the data used by other authors to approximate tidal range) in different parts of the Red Sea, and to variations in local beach profiles. Nevertheless, there are clearly uncertainties in our data about the precise position of shoreline and coral features in relation to mean sea level, and we apply a margin of uncertainty of  $\pm 0.5$  m in our estimates of palaeo sea level from coral terraces, and  $\pm 1.5$  m when using beachrock.

Additional errors, of course, may arise from the erosion of the original surfaces or other irregularities in their surface morphology, an expectation reinforced by variations shown by our data in the measured elevation of different exposures of the same coral platform or beachrock formation in the same locality, and we refer to these in our discussion of the results.

### 3.6 Archaeological Survey

Following the 2014 expedition, a renewed season of archaeological fieldwork, in collaboration with the Saudi Commission for Tourism and National Heritage (SCTH), was undertaken to complete archaeological surveying of the newly-identified terraces that had not been examined in previous seasons of fieldwork (Inglis et al. 2015), the findings of which are included in this chapter.

### 3.7 Geochronology

At the time of writing, the dating samples are still awaiting analysis. We therefore concentrate here on the description of the sample locations, their elevation, and their geomorphological, geological and archaeological implications. We acknowledge that further refinement in estimates of palaeo mean-sea-level would be possible by specifying the species of individual corals selected for dating and their growth position. Since the dating programme is still in progress, however, and given the purposes of this chapter, we do not pursue such refinements here. In any case such refinements need to be weighed against the other sources of uncertainty or error discussed above.

---

## 4 Results

### 4.1 Harrat Al Birk

Thirteen locations were visited along the coastline between the town of 'Amq and just south of the town of Al Qahma (Table 2, Fig. 4). The sedimentary facies present within the terraces varied between locations and included coral, beachrock and finer-grained shell/sand facies consistent with shallow marine deposition.

**Table 2** Palaeoshoreline features in the Harrat Al Birk, showing locations visited and samples taken for dating, details of elevations of palaeoshoreline features and estimates of palaeo sea level. The elevations are given in two forms: (a) the raw data as measured in the field by DGPS above the local sea surface at the time of measurement; (b) the estimated height of mean palaeo sea level above modern palaeo sea level, using the correction factors presented in Table 1 for modern mean sea level, and an additional correction and margin of uncertainty to estimate the elevation of the mean palaeo sea level. See the text for further explanation and discussion

Locality	GPS	Description	DGPS Station name	Measured Elevation of Upper Surface (m above local datum)	Corrected elevations (m amsl)	Palaeo sea level (m amsl)	Margin of uncertainty m	Coral samples (U-series)	Basalt Samples ( <sup>40</sup> Ar/ <sup>39</sup> Ar)	Shells
L0103 (2014-12-05-5)	N 18.405430° E 41.459820°	2 km terrace of beachrock overlying coral, overlying basalt.	North of 'Amq	Beachrock 4.55–5.34	Beachrock 5.05–5.84	Beachrock 4.05–4.84	±1.5	–	–	–
L0078 (2014-12-04-1)	N 18.268010° E 41.514970°	Coral terrace adjacent to present-day shore with shell scatter.	Al Birk Station 2	3.45	4.03	5.03	±0.5	HAB-33 to -35	–	HAB-36 (Tridacna) HAB-37 (surface shells)
L0129 (2014-12-04-2)	N 18.260167° E 41.514550	Weathered coral remnant overlying basalt.	Al Birk Station 2	3.44–3.57	4.02–4.15	5.02–5.15	±0.5	HAB-38	–	HAB-39, -40 (Tridacna)
L0093 (2014-12-04 & -03)	N 18.240180° E 41.528170° & N 18.240183° E 41.528100°	Terrace of sandy/shelly beachrock sediments, coral and broken coral. <i>In situ</i> flake.	Al Birk Station 2	Beachrock 4.87–6.27	Beachrock 5.45–6.85	4.45–5.85	±1.5	HAB-40 (redeposited)	–	HAB-42 (surface shells)
L0090 (2014-12-04-5)	N 18.204086° E 41.524858°	Coral terrace overlying basalt headland at Al Birk.	Al Birk Station 2	3.45–3.88	4.03–4.46	5.03–5.46	±0.5	–	–	–
L0035 (2014-12-4-7 and -8)	N 18.173730° E 41.565170° and N 18.172830° E 41.564740°	Coral terrace remnant overlying basalt.	Al Birk Station 1	3.20–3.50 and 3.30–3.60	3.61–3.91 and 3.71–4.01 m	4.61–4.91 and 4.71–5.01 m	±0.5	HAB-44	–	HAB-43 (Tridacna)
L0036 (2014-12-04-9)	N 18.168730° E 41.566490°	Coral terrace overlying basalt. Heavily bulldozed.	Al Birk Station 1	4.53–4.85	4.94–5.26	5.94–6.26	±0.5	–	–	HAB-45 (Tridacna)
L0038 CASP site 216-208 (2014-12-05-1)	N 18.135010° E 41.578940°	Coral terrace overlying basalt.	Al Birk Station 3	2.96–5.27	3.54–5.85	4.54–6.85	±0.5	–	–	–
L0092 (2014-12-05-2)	N 18.122060° E 41.596840°	1 km exposure of beachrock overlying coral and basalt.	Al Birk Station 3	Beachrock 3.57–6.87	Beachrock 4.15–7.45	3.15–6.45	±1.5	–	–	–
L0034 Dhahaban Quarry (2014-12-05-1 to -7)	N 18.072444° E 41.623544°	Complex of shallow marine, coral and beach deposits overlying cobble unit containing rolled coral heads and sharp artefacts.	Dhahaban Station	Coral 5.09–7.52 Beachrock 5.24–7.81	Coral 5.62–8.05 Beachrock 5.77–8.34	Coral 6.62–9.05 Beachrock 4.77–7.34	±1.5	HAB-010, -012, -013, -015, -016, -026.	HAB-001, 007, 008, 017, 019, 030, 031	–

(continued)

**Table 2** (continued)

Locality	GPS	Description	DGPS Station name	Measured Elevation of Upper Surface (m above local datum)	Corrected elevations (m amsl)	Palaeo sea level (m amsl)	Margin of uncertainty m	Coral samples (U-series)	Basalt Samples ( $^{40}\text{Ar}/^{39}\text{Ar}$ )	Shells
L0091	N 18.066220° E 41.635390°	Sandy conglomerate of shells and coral heads overlain by beachrock and associated with basalt terrace.	Al Birk Station 3	5.93–6.63	6.51–7.21	5.51–6.21	±1.5	–	–	–
L0089 (2014-12-05-4)	N 18.035758° E 41.652261°	Major sequence of partially-bulldozed coral terraces overlain by beachrock and potential aeolianite.	Al Birk Station 3	Coral 3.15–5.81; beachrock 5.81–7.40	Coral 3.73–6.39 Beachrock 6.39–7.98	Coral 4.73–7.39 Beachrock 5.39–6.98	±1.5	–	–	–
L0128	N 17.975367° E 41.684250°	400 m long exposure of beachrock abutting basalt.	Qahmah	5.19–6.32	5.65–6.78	4.65–5.78	±1.5	–	–	–

**L0103**

At 800 m from the present-day shoreline and 6 km south of 'Amq, the southern extent of a ~2 km exposure of beachrock facies overlies heavily-weathered coral (Fig. 5a, b). At its southern extent, the top of the beachrock terrace varies between 5.05 and 5.84 m above mean sea level (all elevations given in this form in the text have been corrected to the local mean sea level). No material suitable for U-series dating was identified in the terrace.

During the 2015 archaeological survey, a single lithic artefact was observed and collected from the beachrock surface, a basalt ESA (Early Stone Age)/MSA core fragment. At the foot of the low, undulating, basalt jebels behind the marine deposits, twenty artefacts made on quartz or basalt were collected, including ESA and MSA cores and flakes, as well as small flakes and cores made on quartz of potential LSA (Late Stone Age) date.

**L0078**

This is 7 km north of Al Birk, where a coral terrace is preserved adjacent to the present-day shore. The top of the coral terrace was measured at 4.03 m (Fig. 5c, d). Three coral samples were removed from the coral deposit, samples HAB-033 to -035, along with a *Tridacna* shell (HAB-36) and a sample of shells from the surface (HAB-37). A thin shell-midden deposit comprising edible marine molluscs collected as food lies on the surface of the terrace and has been radiocarbon dated to  $5560 \pm 70$  BP (Beta-191460); a radiocarbon sample from shell embedded in the underlying coral terrace gave an infinite age (Bailey et al. 2007b). In 2014, six basalt and andesite artefacts were collected from the surface of the terrace, including MSA prepared cores, and flakes struck from prepared cores (Inglis et al. 2014b).

**L0129**

A very weathered and partially damaged remnant of coral terrace overlies a basalt lava flow adjacent to the present sabkha, with its uppermost (albeit degraded) extent measured at 4.02–4.15 m amsl (Fig. 5e, f). A single sample of fibrous coral was recovered (HAB-38) at 2.62 m amsl. Complete and fragmentary *Tridacna* shells were also collected (HAB-39 and -40). No archaeological material was observed.

**L0093**

A beachrock terrace overlying a basalt flow consists of sandy sediments containing redeposited cobbles of coral, broken pieces of smaller coral, and shells (Fig. 5g). Spot heights from the top of the terrace varied between 5.45–6.85 m amsl. A single sample of redeposited coral (HAB-40, 4.22 m) was collected from within the terrace, as well as a sample of shells from the terrace surface (HAB-42). An undiagnostic, sharp basalt flake (HAB-41) was recovered from within the terrace at 4.78 m amsl (Fig. 5h). In 2014 a single MSA basalt flake was observed on the surface of the terrace (Inglis et al. 2014b).

**L0090**

A headland formed by a basalt lava flow extends from the town of Al Birk into the sea. At its tip, and adjacent to the present-day beach, a coral terrace overlies the basalt, but has been heavily damaged by bulldozing. The terrace continues beyond a security fence into a fenced area where it remains intact (Fig. 6a, b). The height of the undamaged terrace was measured at the fence line (closest to its undisturbed height) at 4.03–4.46 m amsl. Suitable material for U-series dating was not identified. In 2014, a single MSA prepared core preform on basalt was found on the surface of the coral terrace (Inglis et al. 2014b).

**L0035**

Overlying a basalt lava flow, coral terrace remnants were preserved adjacent to the modern day sabkha (Fig. 6c, d). At 2014-12-04-7 the top of the terrace was measured at 3.61–3.91 m amsl and a *Tridacna* shell was collected (HAB-43). Suitable coralline material for U-series dating was not identified. At 2014-12-04-8, close by, and probably contiguous with the previous station, the top of the coral terrace varied from 3.71–4.01 m amsl. A large block of coral had been broken off from the terrace by bulldozing, and a sample of fresh-looking coral was removed from this block (HAB-44). Thirty-five basalt flakes and cores, including artefacts with ESA and MSA affinities, were observed on the lava flows above the raised coral terrace, and on the surface of the terrace itself (Inglis et al. 2014b).

**L0036**

A remnant of coral terrace less than half a kilometre to the south of L0035 was surveyed (Fig. 6e, f). The top of the terrace was measured at 4.94–5.26 m amsl. The coral was heavily weathered, and no suitable dating material was located, but a *Tridacna* shell was collected from the terrace surface (HAB-45). In 2013, eighteen MSA and ESA basalt flakes and cores were observed on the upper, disturbed parts of coral terraces overlying the lava flow (Inglis et al. 2014b).

**L0038, CASP Site 216-208**

First recorded by the Comprehensive Archaeological Survey Programme (CASP; Zarins et al. 1981), a coral terrace at this location overlies a lava flow adjacent to the modern sabkha (Fig. 6g, h). It was visited in 2004 (Bailey et al. 2013b) and comparison with photographs in Zarins et al. (1981) showed that considerable damage had already taken place in the interval. Since 2004, much of the immediate locality has been further bulldozed for the construction of a coastguard station, and only part of the coral terrace remained intact as of December 2014. The coral terrace contains two facies, a lower facies of consolidated carbonate and basalt clasts overlain by an upper facies of coral, both in growth position and with a matrix of broken pieces of branching corals. The upper surface of the terrace was measured at 3.54–5.85 m amsl. No material suitable for U-series dating was identified.

Emplacement of the underlying lava flow has been dated by K/Ar to  $1.37 \pm 0.02$  Ma and  $125 \pm 0.02$  Ma (Bailey et al. 2007b). The CASP survey recorded Palaeolithic artefacts with ESA and MSA affinities on the surface of the terrace and underlying basalt. These observations were confirmed by the DISPERSE project, with extensive scatters of ESA and MSA basalt artefacts present on the surface of both sides of the lava flow and coral terrace, including a crude handaxe, radial cores and flakes (Inglis et al. 2014b). Above the coral terrace, an area of SCTH protection

encloses boulders engraved with South Arabic script (~9–5th century BC) and shallow tunnels excavated into the volcanic deposits.

**L0092**

A >1 km-long exposure of weathered coral and beachrock deposits overlies a basalt flow 1.5 km from the present shoreline (Fig. 7a, b). Elevation of the beachrock surface was measured at 4.15–7.45 m amsl. No material suitable for U-series dating was identified. A survey of the exposure yielded eight lithics with MSA affinities, including cores made on basalt and a convergent flake (Inglis et al. 2014b).

**L0034 Dhahaban Quarry**

Initial DISPERSE reconnaissance in May 2012 identified marine deposits exposed in a modern quarry section close to the coastal road, overlying the basalt flow from an adjacent cinder cone (Devès et al. 2013). Further geoarchaeological investigations were undertaken in 2013 (Inglis et al. 2013). This site is of particular importance because of the number of artefacts that have been recovered here. Many are on the surface of the marine deposits but there are also 19 stone tools in sharp and unrolled condition found stratified within a water-laid cobble unit underlying a complex series of beach, shallow marine and aeolian deposits (Inglis et al. 2014b; Bailey et al. 2015). Because of quarrying activity and erosion by stream action that has cut a wadi bed through part of the deposits, there is no single exposure where the full sequence of deposits can be seen in one section, complicating the task of unravelling their stratigraphic relationships (Fig. 8).

The major depositional units are as follows:

**In situ Coral Terrace.** These deposits extend to the north of the locality, including large coral heads and facies of broken coral (Fig. 9a, b). Quarrying activity, wadi incision and other disturbances have removed parts of this unit, which is now preserved in several spatially discrete areas (Fig. 8). From the appearance and condition of these coral terrace fragments, their spatial configuration, and their surface elevation, we consider that they are parts of the same unit formed during the same sea-level episode. The upper surface of this coral terrace varies between 5.62 and 8.05 m amsl with large coral heads observed in growth position at 3.78 m amsl in the bulldozed area to the north of the wadi cut, opposite the cobble unit exposure. MSA stone tools are present in places on the surface, especially near the north bank of the present-day stream bed.

**Beachrock.** This is present mainly in the central and southern area of the locality, but also in fragments overlying coral in the northernmost extent of the exposed deposits (Fig. 9c). The upper surface of the beachrock varies between 5.77 and 8.34 m amsl. Some of the beachrock is located at a

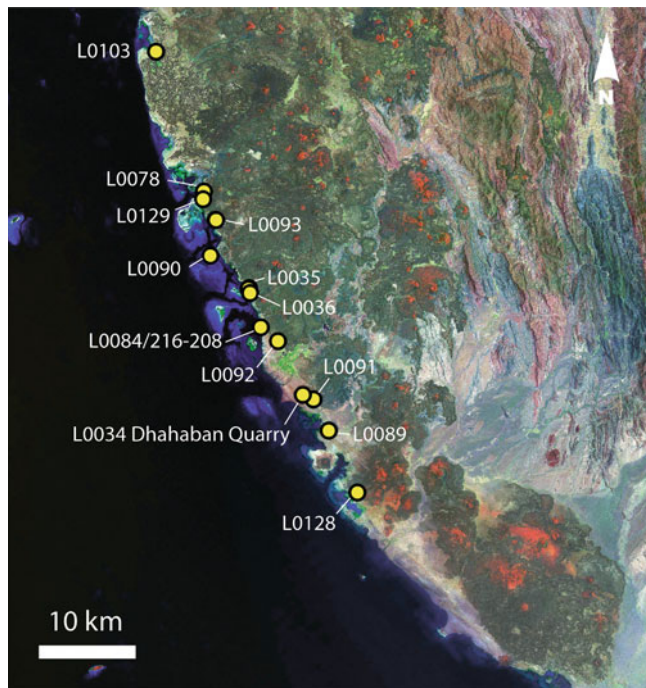


**Fig. 4** Locations of marine terraces surveyed and sampled in the Harrat al Birk. Satellite imagery © USGS Landsat ETM + 200 Geocover Mosaics. The orange patches are volcanic cinder cones and the dark green areas are basaltic lava flows

higher elevation than the coral terrace and stratified above it, as would be expected if they belonged to the same sea-level episode. However, some beachrock is lower than the highest points of the coral terrace, suggesting at least two different episodes of high sea level, or a period of variable sea level within an interglacial period, with at least some of the beachrock deposited during marine regression. MSA stone tools are present in places on the beachrock surface.

**Cobble Unit.** A unit of rounded pebbles, cobbles, re-deposited coral heads and occasional mollusc shells including a large oyster shell. The unit is restricted to a small area where the wadi drains the *harrat* behind the quarry and has exposed the cobble unit in a section extending for about 20 m along the southern margin of the wadi, where it is overlain by lithified shallow marine sands and beachrock (Fig. 9d). The upper limit of the unit, at the contact with shallow marine sands/beachrock, slopes between 7.74 to 7.34 m amsl, with its lowest exposure from 6.02 to 5.2 m amsl at the edge of the present wadi bed; the unit probably extends deeper. The cobbles are highly variable in size ranging from <5 cm up to 30 cm in maximum dimension. They consist of heavily rolled pieces of basalt that have clearly been derived from the basaltic bedrock immediately inland. The deposit has the appearance of a debris flow deposited by torrential stream action. Nineteen sharp basalt

flakes were collected from this unit. The fact that they show no evidence of rolling or abrasion, unlike the rest of the clasts, suggests that they have not moved far from their original discard location. Samples from five coral heads were also removed from this unit, including a large coral head oriented in growth position, but not necessarily in primary position.

**Marine Sands.** Silty sand and shell sand facies exposed in a quarry cut ~6 m deep at the southern end of the site and capped by aeolianite (Fig. 9e); the top of this section is at 8.74 m amsl, with the transition between aeolianite and marine/beach sediments at ~1.25 m below the top of the section (~7.49 m amsl). Samples were removed from this section in 2014 and 2015 for OSL dating at the Scottish Universities Environmental Research Centre, UK (Sanderson and Kinnaird, this volume).

**Aeolianite.** At the southern end of the site, cemented aeolian deposits abutting the slopes of the cinder cone, and directly overlying the shallow marine sediments in the main quarry section, were observed extending up to at least ~23 m amsl on the volcanic cone. (Fig. 9f).

Analysis of the complex depositional history at Dhababan Quarry and its implications for reconstructing sea level change is ongoing. The main sequence of events from earliest to latest appears to be as follows: (a) formation of a volcanic cinder cone and associated lava flows at some indeterminate stage in the Pleistocene; (b) marine transgression followed by formation of coral, deposition of shallow marine sands and formation of beachrock deposits during one or more high sea-level stands; (c) accumulation of wind-blown sands derived from the exposed sea bed during the subsequent marine regression, and later cemented through carbonate precipitation into aeolianite.

The most difficult unit to place in this sequence is the cobble unit. We consider three hypotheses:

- A storm deposit formed at the back of a beach broadly coeval with the coral terrace and beachrock formations and part of the same high sea-level stand.
- A fluvial unit accumulated before the high sea-level stand associated with the coral terrace and beachrock formations, based on the fact that the cobble unit is stratified beneath an overlying beachrock deposit and is at a lower elevation than the adjacent coral terrace on the opposite bank of the wadi.
- A fluvial unit formed during an interval of minor sea-level regression and incision of the stream bed between an earlier high sea-level stand associated with the coral terrace and a later high sea-level stand of similar or slightly lower elevation associated with the overlying beachrock.

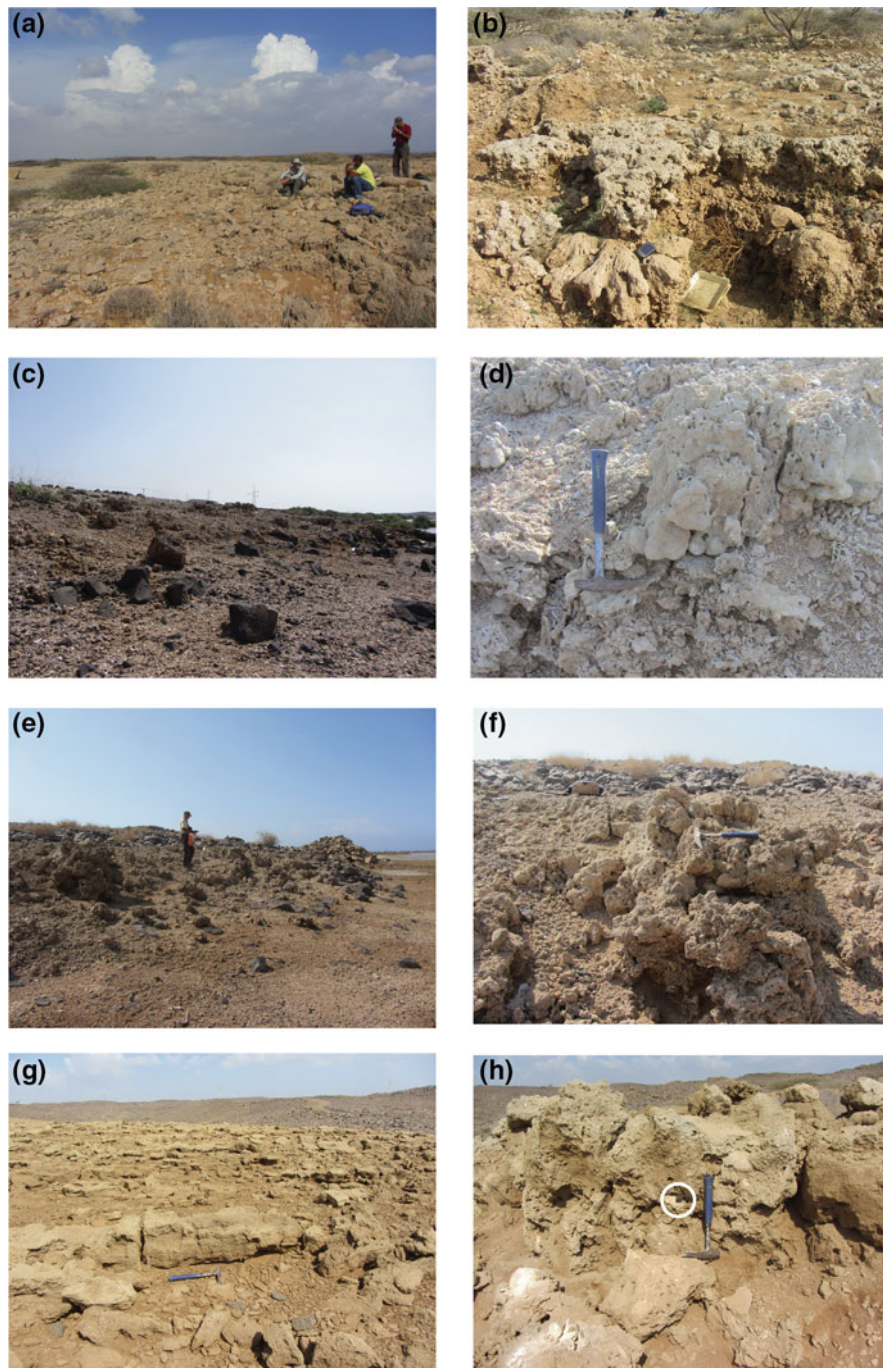


**Fig. 5** Views of marine terraces surveyed in 2014 (1): **a, b** L0103 beachrock overlying heavily-weathered coral; **c** L0078 coral terrace overlain by shell scatter, and coral sampled (**d**); **e, f** L00129 heavily weathered coral terrace remnant overlying basalt; **g** sandy sediments with broken coral and shell at L0093 with **h** worked basalt flake removed from deposits to left of centre of geological hammer (circle marked). Photos: Robyn Inglis, December 2014

We reject (a) on the grounds of the highly variable clast size, the lack of sorting, the thickness of the deposit, its alignment along the line of the wadi, and the fact that it contains well-embedded within it stone artefacts with sharp edges that show no signs of rolling or water abrasion (Fig. 10).

Hypothesis (b) is possible, but we then have to explain the source of the coral heads embedded in the cobble unit and to suppose that they were eroded from a coral terrace formed during an earlier period of high sea level. There is no evidence for such a coral terrace in the vicinity, nor any evidence that the coral terrace deposits at the site are of

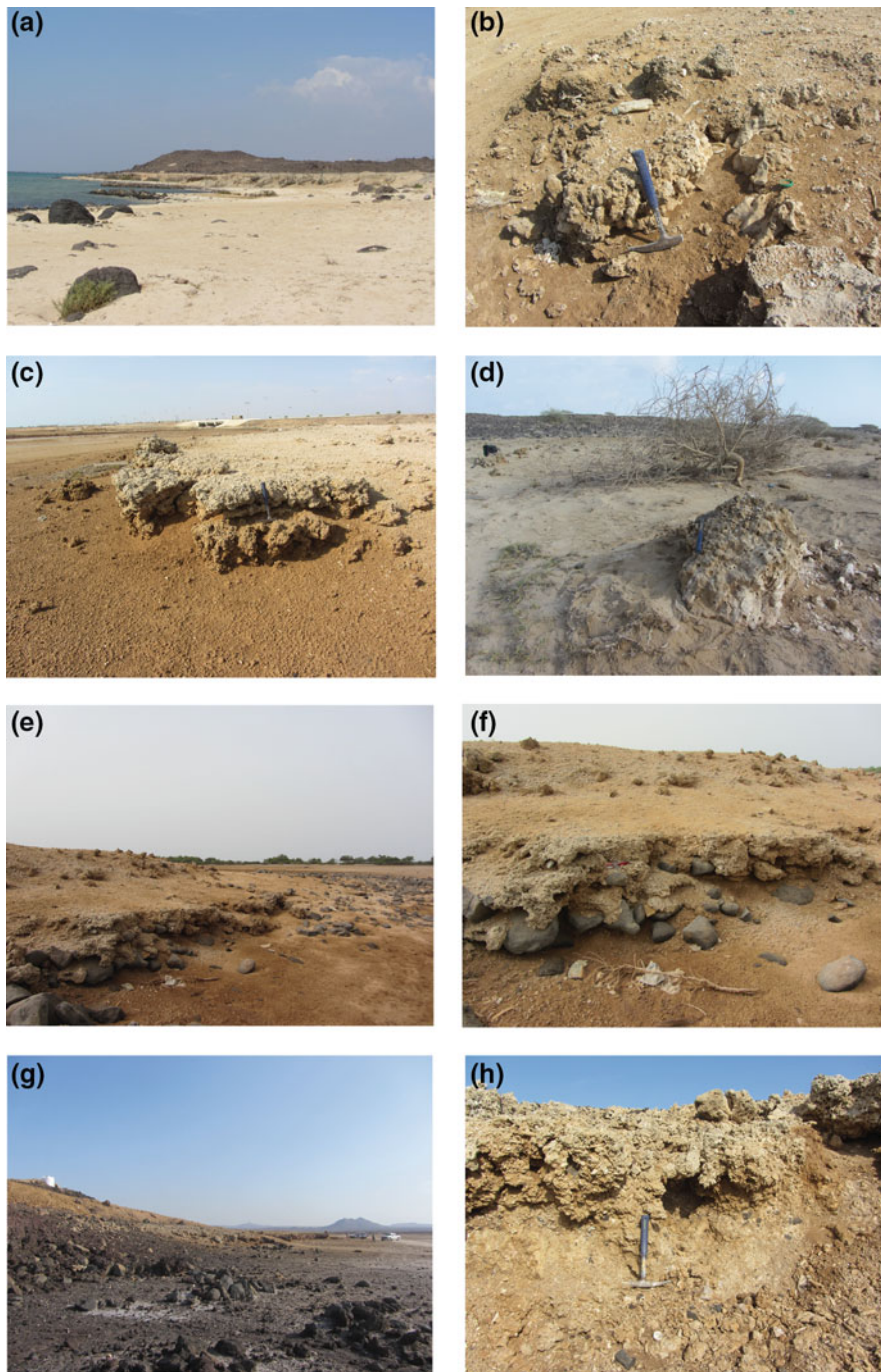


**Fig. 6** Views of marine terraces surveyed in 2014 (2): **a, b** partially-bulldozed coral terrace overlying basalt at end of Al Birk headland; **c** coral terrace remnants adjacent to sabkha at L0035, and **d** sampled block of coral from terrace; **e, f** coral terrace remnant overlying basalt at L0036; **e, f** partially bulldozed coral terrace at L0038, CASP site 216-208. Photos: Robyn Inglis, December 2014

composite structure, formed of coral deposited during two periods of sea level separated by  $\sim 100$  kyr (e.g., evidence of unconformity or differences in the condition and degradation of the coral). But, these observations are not decisive.

Hypothesis (c) is also possible, and would account for the presence of the coral heads and marine shell found within the cobble unit, as well as the corals observed in growth

position as low as 3.78 m amsl exposed in the bulldozed area of the wadi. Minor oscillations of eustatic sea-level are recorded within MIS 5e and are consistent with this hypothesis (see Rovere et al. 2016, and references therein). We consider association of any of the observed palaeoshoreline features with the high sea-level stands of the later stages of MIS 5 as unlikely because these were formed

at sea levels some 20 m lower than the MIS 5e sea level. For the moment, we consider this the most likely hypothesis, while emphasising that a decisive test in its favour in preference to (b) will be a demonstration by U-series dating of broad contemporaneity between the large coral heads within the cobble unit and the adjacent coral terrace.

From the archaeological point of view, both hypotheses (a) and (c) imply a significant episode of human activity on or very close to shoreline of the contemporaneous sea coast, whereas under hypothesis (b) the cobble unit and its embedded artefacts could have been deposited at any period in the sea level cycle, including a period of marine regression when the coastline was located many tens of kilometres to the west.

#### L0091

A small coral terrace 1 km to the east of the Dhahaban Quarry, overlying the same basalt flow, was preserved in the mouth of a wadi draining the *harrat* (Fig. 7c, d). The terrace consists of a conglomerate of shells and coral heads, some in growth position. This was overlain by a beachrock facies, the upper surface of which was coincident with a break in slope in the lava terrace that continued to the east. The top of the beachrock was measured to between 6.51–7.21 m amsl. Mangrove whelks and gastropods were observed in and on the sediments. No material suitable for U-series dating was identified in the terrace. In 2014, a potential ESA handaxe roughout on basalt and a rolled basalt clast with retouch were observed on the basalt (Inglis et al. 2014b).

#### L0089

An eroded cinder cone and its surrounding basalt flows to the west of the coastal road, isolated from the main *harrat*, are overlain on their northwestern and western flanks by a complex of coral terraces, beachrock and aeolianite (Fig. 11). In places, the coral terraces (which have been subject to some bulldozing and disturbance) contain >1 m coral heads in growth position. Profiles were measured from the top of the largest of these exposures to the *sabkha* at the foot of the terrace. The surface of the coral, partially bulldozed in places, varies between 3.73 and 6.39 m amsl, with the surface of the beachrock between 6.39 and 7.98 m amsl. No material suitable for U-series dating was identified in the deposits. In 2014, 13 artefacts with MSA affinities, manufactured in basalt, quartz and andesite, were collected from the surface of these deposits, mainly the beach rock surfaces, including prepared cores and points (Inglis et al. 2014b).

#### L0128

South of Al Qahma, a 400-m long exposure of beachrock, 500 m inland from the present shoreline, overlies a basalt lava flow (Fig. 7e, f). Part of the beachrock has been quarried, leaving large piles of boulders of the material. The

intact surface of the exposure was measured to between 5.65–6.78 m amsl. Numerous funerary cairns, some of relatively recent origin, have been built on the beachrock terrace and surrounding basalt hillsides and pottery was found on the surface of the beachrock.

## 4.2 Farasan Islands

Three days of surveying were spent on the Farasan Islands, targeting three principal areas (Fig. 12):

- (1) The north of Farasan Al Kabir, the largest island of the Farasan group, near the village of Sair and the fishing village of Al Hussain. This area shows obvious signs on satellite images of tectonic uplift associated with salt tectonics.
- (2) The Sulayn and Abalat group of islands, north of the main port on Farasan al Kabir.
- (3) Ras Sheida, near the southern extremity of Farasan al Kabir.

The surface geology of the Farasan Islands is dominated by highly-faulted cemented coral reef terraces, often described as ‘limestone’, and intervening depressions floored by modern, fine-grained alluvium (Fig. 13). The limestone units have been collectively referred to as the ‘Reef Limestone’ (Macfadyen 1930) or ‘Farasan Island Limestone’ (Bantan 1999) and based on limited U-series dating all are of Pleistocene date and in some cases Holocene (Bantan 1999). Bedding dips are generally horizontal to very shallow but locally attain  $\sim 30^\circ$ . Their maximum elevation is now  $\sim 75$  m asl, but most of the coral terraces lie at 20 m or less. Many of the terraces are cut by pronounced open linear fissures and metre-scale grabens that generally parallel nearby faults (Fig. 14). Both these secondary structures are indicative of predominantly horizontal extension without any evidence of significant strike-slip movement.

Shallow-well data summarized in Bantan (1999) demonstrate that the surficial reef limestones attain a maximum thickness of at least 125 m and are underlain by 10–54 m of interbedded gypsum, claystone and marl. Beneath this interbedded sequence there is at least 155-m thickness of massive evaporite (halite) on Farasan al Kabir. At nearby Zifaf Island (Fig. 12) the halite is more than 350 m thick (Macfadyen 1930). The depth to the base of the halite has not been determined in any published well records. Regional correlations suggest that the massive halite beds are Middle to Late Miocene in age.

In addition to the extensive faulting, the stratigraphy of the island is also locally gently folded. This produces kilometre-scale closed and open basins and domes that are best observed in satellite imagery (Bantan 1999). Large

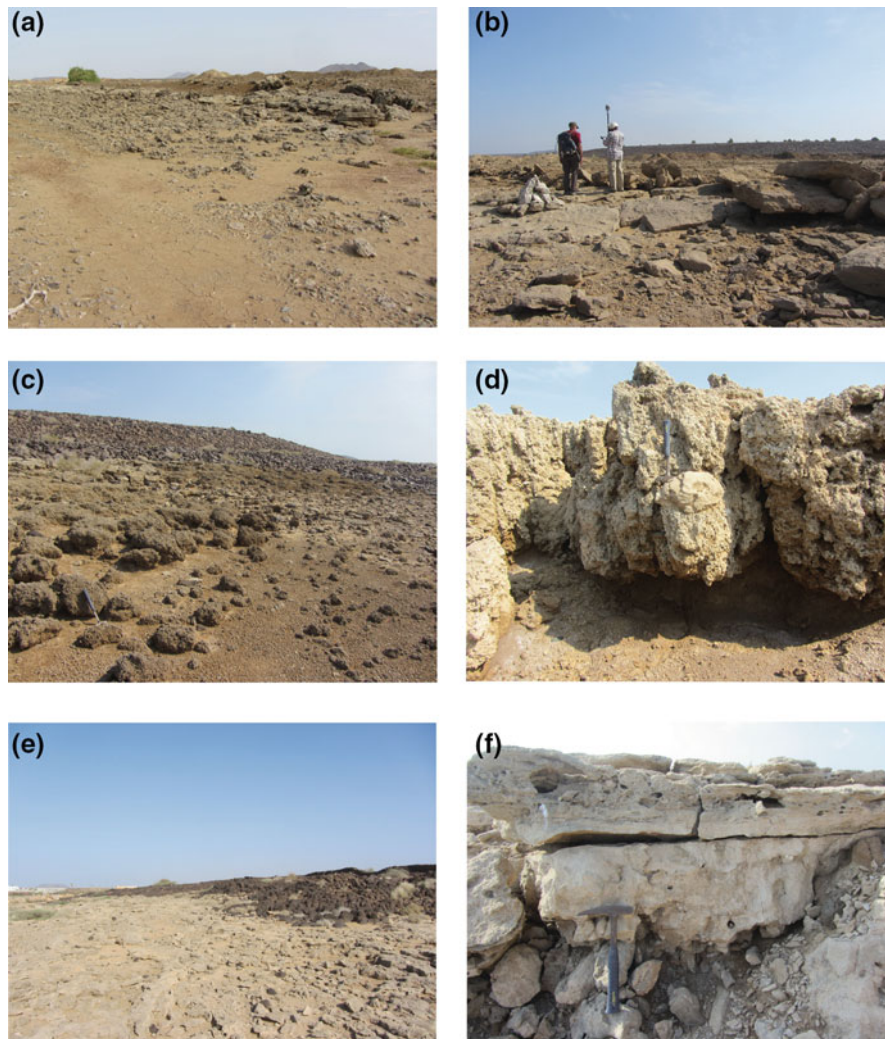


**Fig. 7** Views of marine terraces surveyed in 2014 (3): **a, b** weathered beachrock overlying coral terraces at L0092; **c, d** coral terrace overlying basalt at L0091; **e, f** beachrock overlying basalt at L0128. Photos: Robyn Inglis, December 2014

circular structures are also given expression in much of the shoreline geometry, such as at Al Homrah Bay and Mandhar (Fig. 12). Smaller circular and elliptical depressions with tens to hundreds of metres dimensions occur sporadically across Farasan al Kabir. Examples are seen just east of the hamlet of Al Hussain (Fig. 13). The formation of these circular geomorphological features and the associated gentle folding have been attributed to flow of the underlying Miocene salt (halite) beds (Bantan 1999). This is supported by the fact that the thickness of the post-salt stratigraphic column is highly variable in the drilled wells.

## 5 The North of Farasan al Kabir

Northwest of the village of Seir at Jabal Sudain, coral deposits have been uplifted to  $\sim 15$  m asl. Bantan (1999) measured 12 m of dolomitic and highly fossiliferous

packstone and wackestone overlain by a cap of cemented coral reef. The promontory is bounded by several faults striking ENE–WSW and dipping  $\sim 55$ – $70^\circ$  to the north and south. This location is significant because several of the faults bear well-defined slickenlines that demonstrate largely dip-slip extensional movement. Most faults cutting the Pleistocene limestones elsewhere do not display kinematic indicators.

On the coast to the southwest of the village of Al Hussain there is a bay used by the local fishermen. Immediately behind the modern shoreline is a narrow coral terrace some 3 m in height with a notch formed by marine erosion (Fig. 14, Table 3). This coral platform is typical of the coastal geomorphology found around many of the other coastlines of the Farasan Islands and often has shell mounds located on it (Fig. 3). Behind this terrace is a partly eroded cliff 25–34 m high forming an impressive sequence of uplifted sediments composed of thick deposits of white

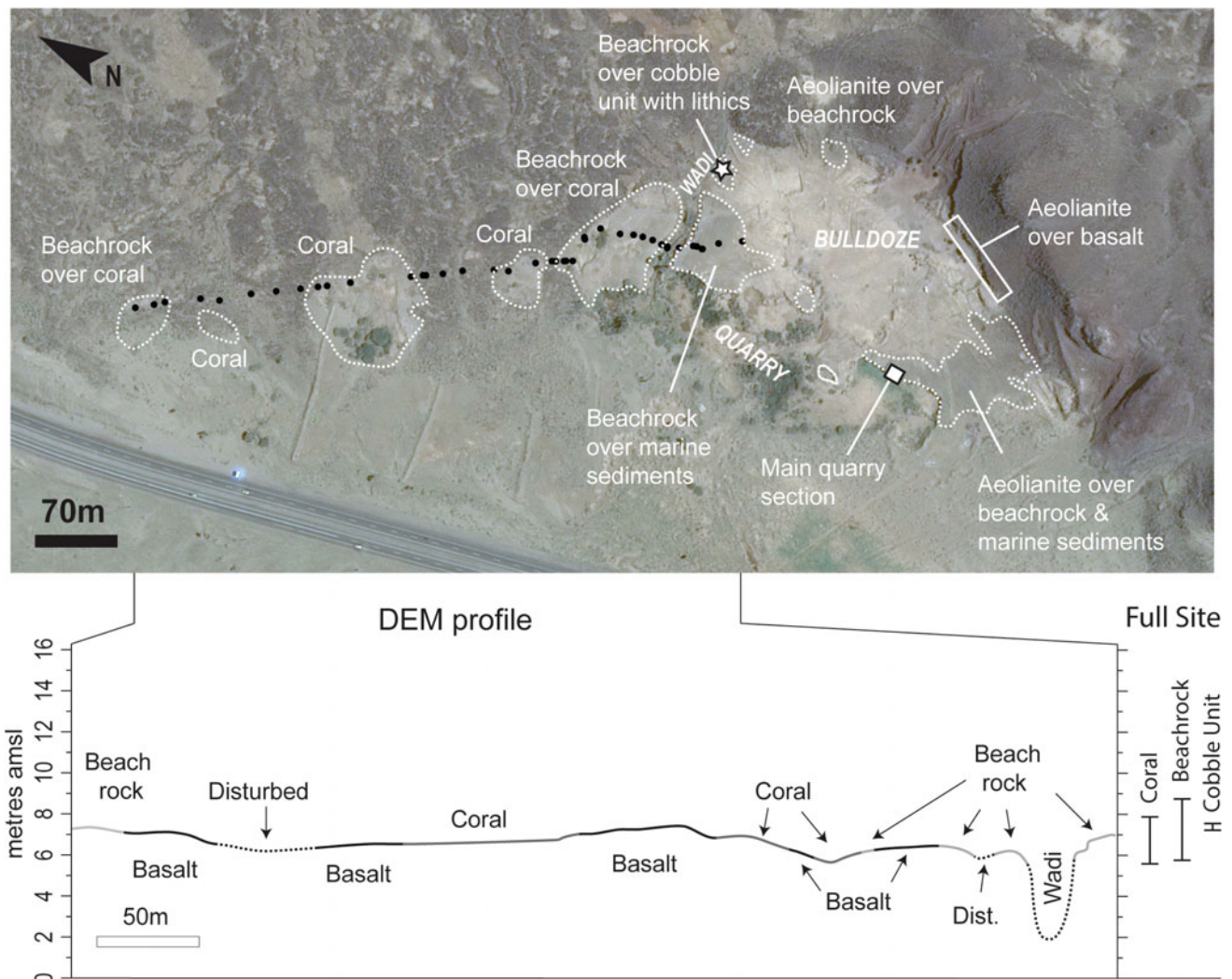


**Fig. 8** Aerial view and elevation profile of sediments at Dhahaban Quarry (L0034). Image © Google Earth, dated 19/01/2014. The DEM profile, surveyed in December 2014, has been expanded horizontally for the sake of clarity. The black dots indicate the line of the DEM profile and the individual measurement stations. Black dotted lines in the DEM profile indicate lack of information because of modern disturbance or accumulation of recent sediments that have obscured the original profile of the wadi and the lower sections of Pleistocene deposits that formed the original wadi infill. Alongside the DEM profile is displayed the full range of the upper surface of key stratigraphic units, surveyed using a total station in 2014. See text for further details

biogenic/bioclastic marine sediments with occasional red banding, the whole sequence capped by a coral reef deposit 2 m thick, which we sampled for dating (16.71686°N; 41.90857°E; Fig. 14). The surficial appearance of this uplifted terrace is not significantly different from the lower-lying terraces.

## 6 Sulayn and Abalat Islands

Most of the smaller islands surrounding Farasan al Kabir display coral terraces at varying, generally relatively low elevations. At Abalat Island a taped spot elevation of the well-developed terrace was 9 m asl (16.80606°N; 42.18356°

E). The topography at Am Murabaah is more complex with a terrace at about 8 m asl (16.73954°N; 42.20501°E) and a higher terrace at about 13 m asl (16.74007°N; 42.20469°E). Each of these sites was sampled for U-series dating (Fig. 15).

## 7 Ras Sheida

Along the present-day coast of Janaba Bay, the modern shoreline is backed by a low coral-reef platform about 2–3 m above present-sea level, which has been undercut by marine erosion, and upon which there are numerous shell mounds of mid-Holocene date.

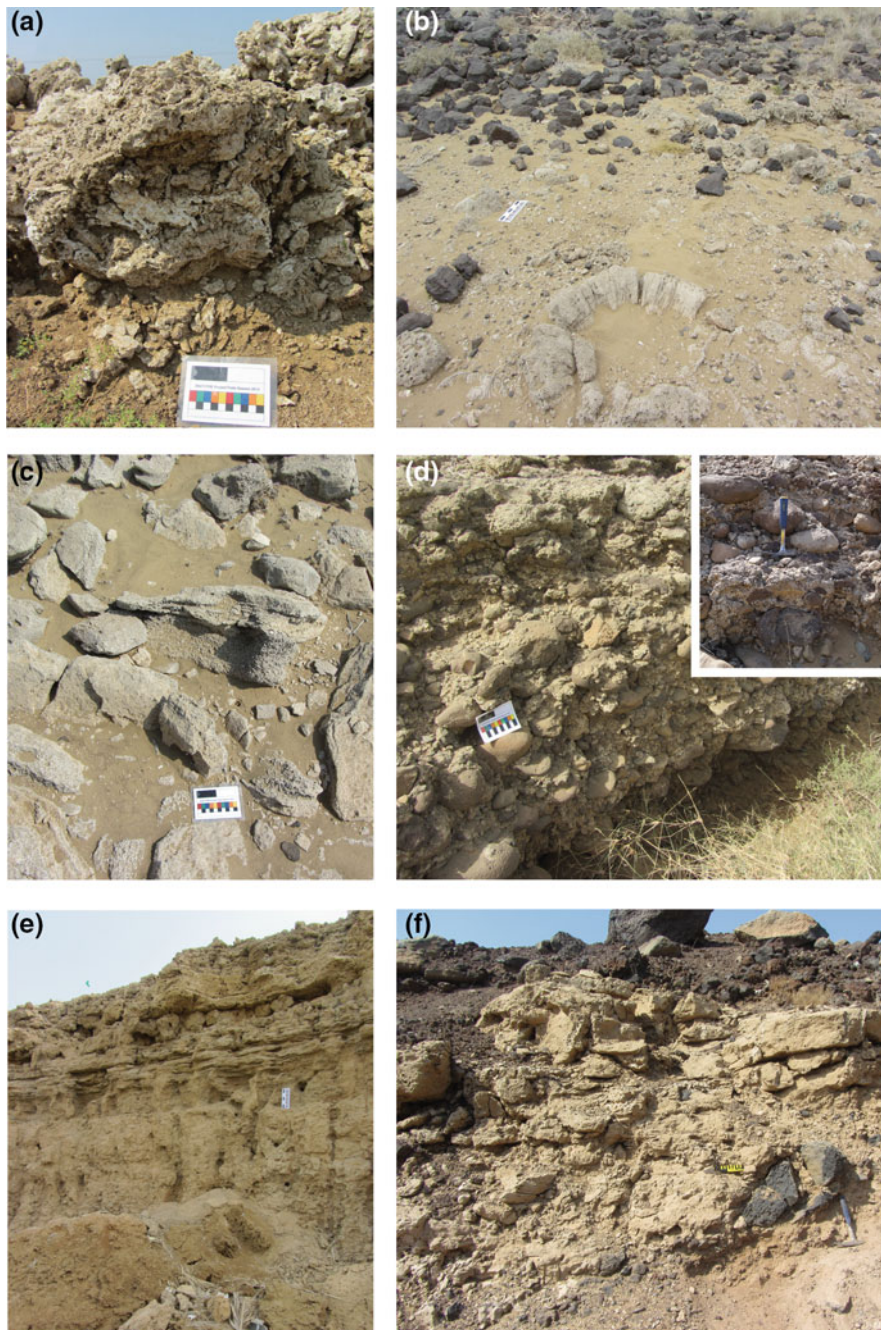


**Fig. 9** Sediment and coral facies at Dhahaban Quarry: **a** coral in growth position in terrace of broken coral; **b** large coral in growth position, partially buried by sediment; **c** beachrock weathering and fragmenting in situ; **d** cobble unit beneath marine sediments containing sharp basalt lithic artefacts as well as rounded coral heads (inset); **e** series of shallow marine sediments capped by aeolianite exposed in quarry; **f** aeolianite overlying scoria and basalt jebel. Photos: Robyn Inglis, December 2014

Ras Sheida, at the southern extremity of Farasan al Kabir, contains a series of four uplifted coral platforms (Fig. 16). The highest is Jebel Sheida, the crest of the reef/terrace standing at 26 m (Fig. 17). Several terrace levels below this can be recognised, but their age relationships are complex and require age dates to ascertain (Table 3).

The 3 m terrace is evident at many locations and may be the MIS 5e terrace. The photograph in Fig. 17 is taken from a position where elevations are generally about 7 m—this could be another candidate for MIS 5e or it could be a degraded older terrace. The ‘gently dipping terrace’ shown in Fig. 17 lies generally at about 10–11 m but does not

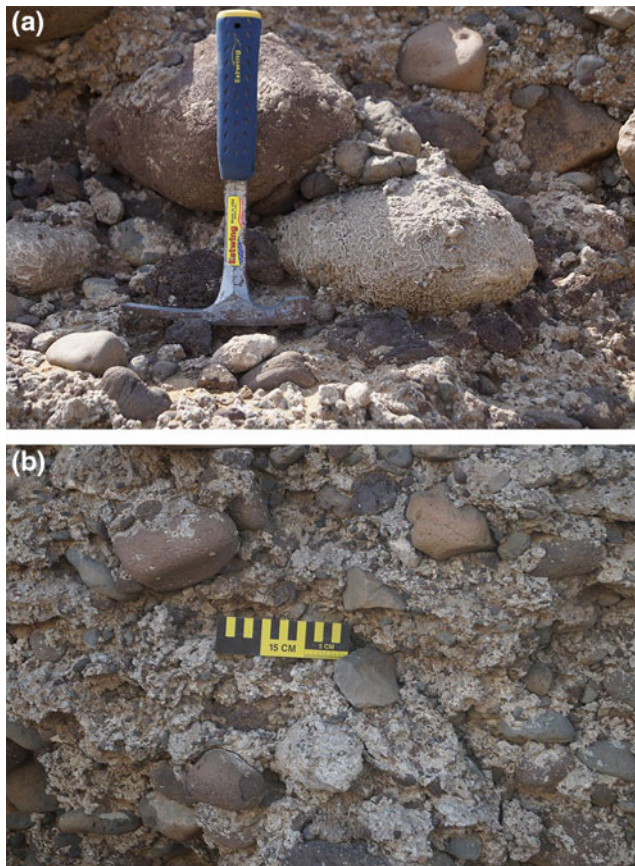


**Fig. 10** Close-up views of cobble unit at L0034 Dhahaban Quarry: **a** basalt cobbles and coral head showing range of sizes; **b** stone artefact in section (to lower right of scale). Photos: Geoff Bailey (a); Bill Bosworth (b), December 2014

connect physically with the 11-m notch on the southern coast. Rather it projects up higher in the structure to about 18 m. Near the south coast, the average dips in the higher carbonate beds are about  $3^\circ$ . This probably reflects footwall uplift/rotation of a fault running along the south side of the Jebel Sheida. Evidence in support of this is that the beds flatten out to the north away from the fault.

## 8 Discussion

Whilst the results from the absolute dating have not yet been obtained, the field observations collected have allowed the development of a set of working hypotheses related to the position of past shorelines in the region surveyed, and their implications for understanding tectonic movement and archaeological evidence of coastal activity.

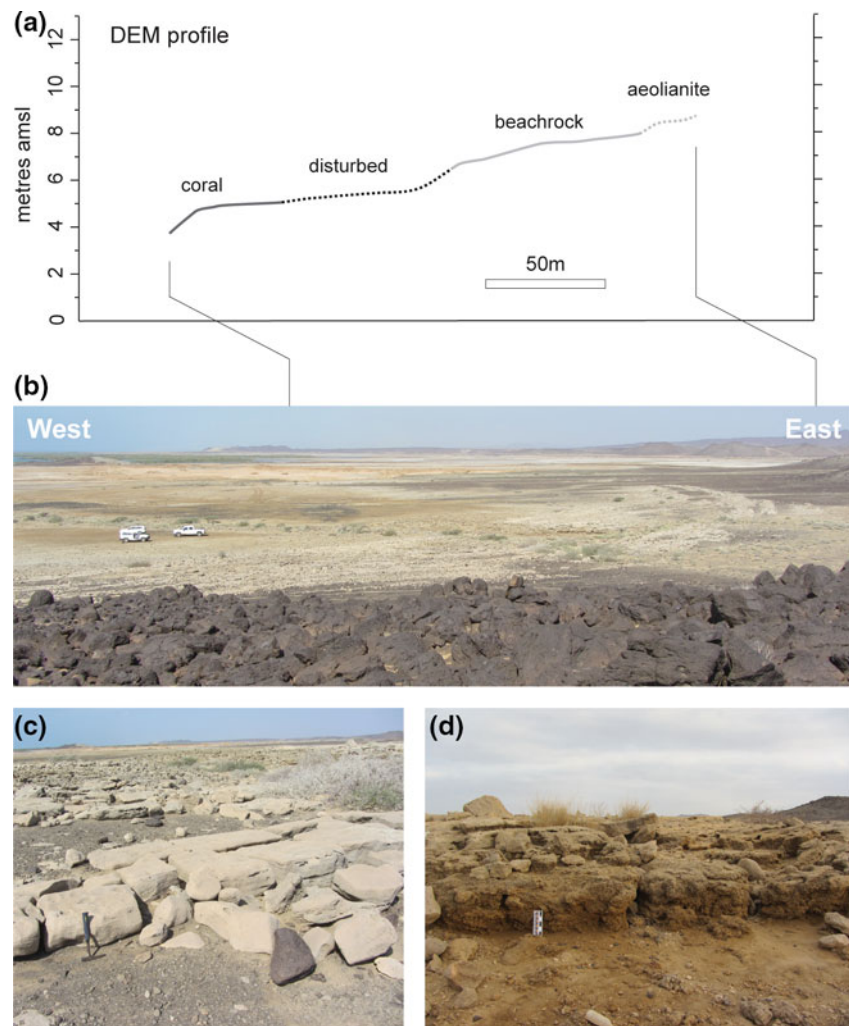
### 8.1 Geological Discussion

The shallow marine deposits, coral terraces, and beachrock occurrences that we have observed in the Harrat al Birk coastal province all presently lie at elevations of  $\sim 3.0$ – $8.5$  m although the upper surface of the Dhahaban Quarry beachrock remains slightly undefined (Fig. 18). In general, beachrock sits at elevations slightly higher than nearby coral terraces, and both overlie the shallow marine units when they are exposed; in many cases beach deposits directly overlie coral terrace deposits. Taking account of the corrections for mean sea level discussed earlier, the maximum palaeo sea level estimate from the study is 9.05 m asl  $\pm 0.5$  m (coral at Dhahaban Quarry), with the rest of the estimates lying between  $\sim 5$  and 7.5 m, subject to errors of up to  $\pm 1.5$  m. In light of this, the 9.05 m coral at Dhahaban Quarry may merit closer inspection and confirmation of its ‘in situ’ setting.

We do not yet have absolute ages for our coral terraces or their associated near-shoreline deposits. However, we can compare our elevations with dated examples from other parts of the Red Sea. Hoang and Taviani (1991) determined U-series dates of 126–138 ka (3 samples) for a coral terrace on Zabargad Island that sits 6–8 m asl. Ages of 125–135 ka (3 samples) were also found for the coral terraces on nearby Rocky Island and North Brother Island in the northern Red Sea (Hoang and Taviani 1991). These terraces have similar elevations of 6–8 m asl. On the Saudi Arabian coastline near Duba, coral terraces dated 119–123 ka (4 samples) are at 4–5.5 m asl (Manaa et al. 2016). On the corresponding Egyptian margin from near Hurghada to Marsa Alam, a coral terrace consistently located at  $\sim 6$  m asl produced a broader range of ages of  $\sim 87$ –131 ka (10 samples; El Moursi et al. 1994), but this is clearly the MIS 5e highstand. Lambeck et al. (2011), referring to a larger dataset, note that MIS 5e elevations of coral reefs lie in the range of 5–9 m with a mean of  $7 \pm 1.5$  m, except in areas of known tectonic deformation and uplift.

These results give elevations similar to our own data. The simplest interpretation of our dataset, then, is that the beachrock at L0093, L0092, Dhahaban, L0091, L0089, and L0128 represents the geographic position and elevation ( $\sim 6$ –7 m above present sea level) of the MIS 5e shoreline. The associated coral deposits were formed near this shoreline, at approximately the same elevation or perhaps 1–2 m lower if they are not the true reef-crest. Further investigation at Dhahaban will elucidate whether the deposits there were deposited by a single high sea stand/cycle, or whether the corals reworked in the cobble unit date from an earlier high sea stand. Our simple and preferred single-high-stand model

**Fig. 11** Profile and photos of coral and beachrock sediments from L0089: **a** DEM profile across centre of coral and beach deposit complex (**b**); **c** beachrock at L0089; **d** coral terrace deposits. Photos: Robyn Inglis, December 2014



for the Harrat al Birk localities is compatible with this limited regional information.

Worldwide, eustatic sea level during MIS 5e is thought to have ranged between +3 and +7 m above the present (Kopp et al. 2009; Benjamin et al. 2017). On the face of it, data from the Red Sea including our results presented here appear to be consistent with this figure, and therefore to indicate either vertical stability or very minor tectonic subsidence in the central and northern Red Sea over the past ~125 kyr.

However, as Lambeck et al. (2011) point out, coastlines are subject to significant changes in elevation as a result of glacio-isostatic and hydro-isostatic effects resulting from the mantle response to re-distribution of loads on the Earth's crust caused by changes in the volume of ice and water, and these effects are likely to show significant geographical variation. These effects can be modelled mathematically and need to be extracted from the elevation of palaeoshoreline indicators before interpretation of the tectonic signal. Detailed modelling by Lambeck et al. (2011) predicts that the position of eustatic sea level in MIS 5e throughout much

of the Red Sea should be close to present sea level assuming an absence of vertical tectonic movement. If that is correct, then the presence of MIS 5e palaeoshoreline indicators at 7 m above present sea level is not evidence of tectonic stability, but evidence of uniform tectonic uplift of about that amount over the past 125 kyr. This in its turn raises questions about the nature of tectonic deformation in different parts of the Red Sea Basin. These may require further investigation of regional tectonic deformation or revision of the assumptions underlying the isostatic model, but further discussion of these issues lies beyond the scope of this chapter.

In the Farasan Archipelago the situation is more complex because of the effects of salt tectonics. The influence of movement of the underlying salt bodies is evident from both satellite imagery (Figs. 12 and 13) and field structural observations. Present-day terrace elevations will therefore reflect the complex interaction between eustatic sea-level changes, regional isostatic and tectonic processes, and local halokinesis. Although eventual determinations of

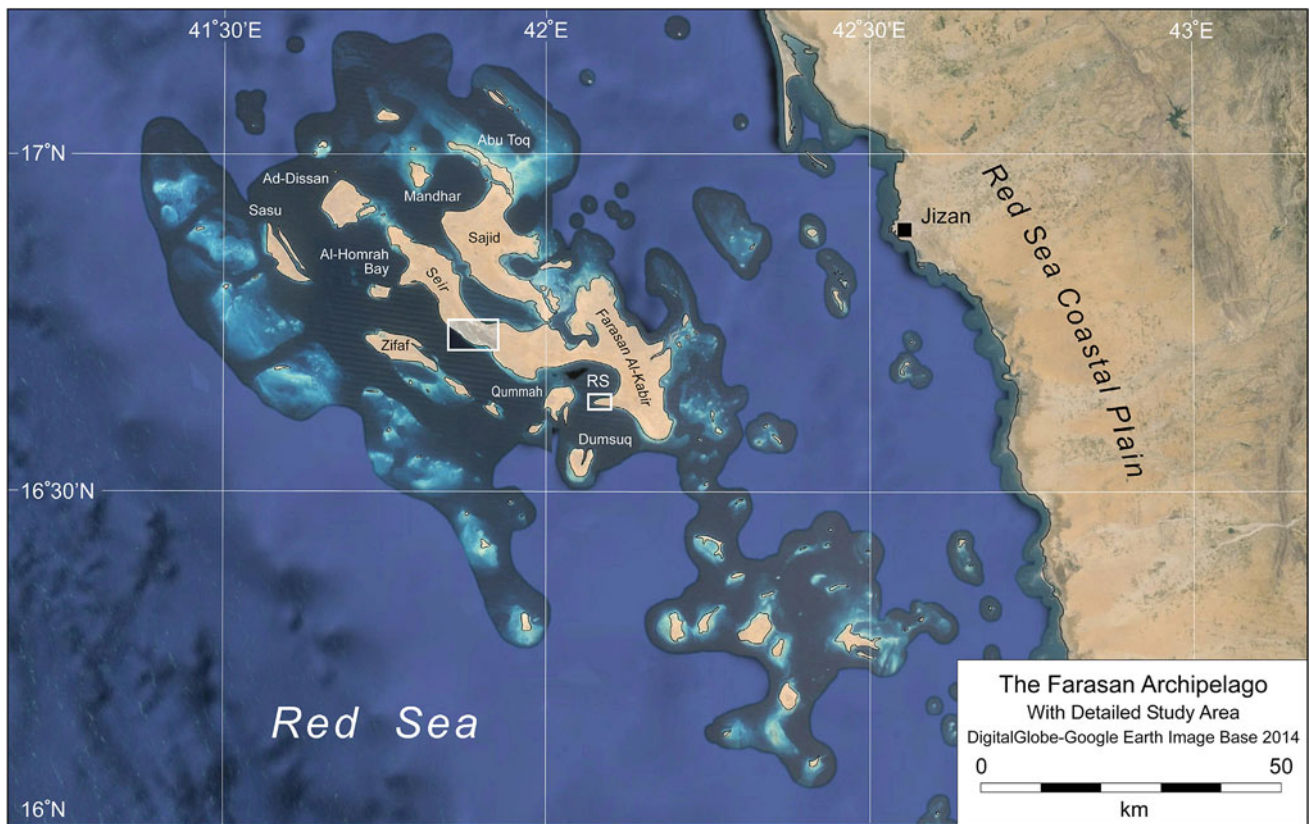


**Fig. 12** Farasan Location Map. Figure 13 location is the box below 'Seir' of Farasan al Kabir. RS = Ras Sheida (see Fig. 15)

uplift/subsidence rates will have mostly local significance, they may help to define when salt movement began in this region and whether its movement was constant through time or varied. Detailed interpretation of the vertical tectonic history here must await radiometric dating of the ages of each of the observed coral terraces.

## 8.2 Archaeological Discussion

Because so much of the archaeological data in our study region comprise stone artefacts lying on the surface with an unknown and uncertain age relationship to their underlying deposits, linking the presence of stone tools to a contemporaneous coastline is problematic. However, two locations in the Harrat al Birk provide the best evidence to date of potential exploitation of the coastline by Palaeolithic populations. At L0093, the presence of a sharp basalt flake embedded within the beachrock terrace indicates that it had been deposited on the beach with little or no geomorphological transport or weathering and surface exposure (either of which would round the flake's edges). It therefore provides a direct link between human activity and beach

sediments, indicating the presence of human activity in the immediate coastal zone.

The stratified artefacts at Dhahaban quarry pose a more complex picture of the relationship between artefact deposition and marine environments. This site is of particular interest and importance not only because it is one of the very few sites in the region where MSA stone artefacts are in a stratified and potentially dateable deposit. It has also yielded one of the largest concentrations of stone tools in the wider region, suggesting that the locality had unusual attractions for human exploitation. Most of these stone tools, of course, are on the surface of the coral terrace. Like the artefacts stratified in the cobble unit, they are mostly of MSA type, although we cannot be sure that they all belong to the same time interval. Nevertheless, their unusual abundance is suggestive.

We have outlined the alternative hypotheses about the interpretation of the cobble unit within which the stratified artefacts occur, and we emphasise that a final interpretation must await the outcome of the dating programme currently underway. Our preferred hypothesis is that the cobble unit formed at or close to the time of the high sea-level stand indicated by the elevated coral terrace and beachrock

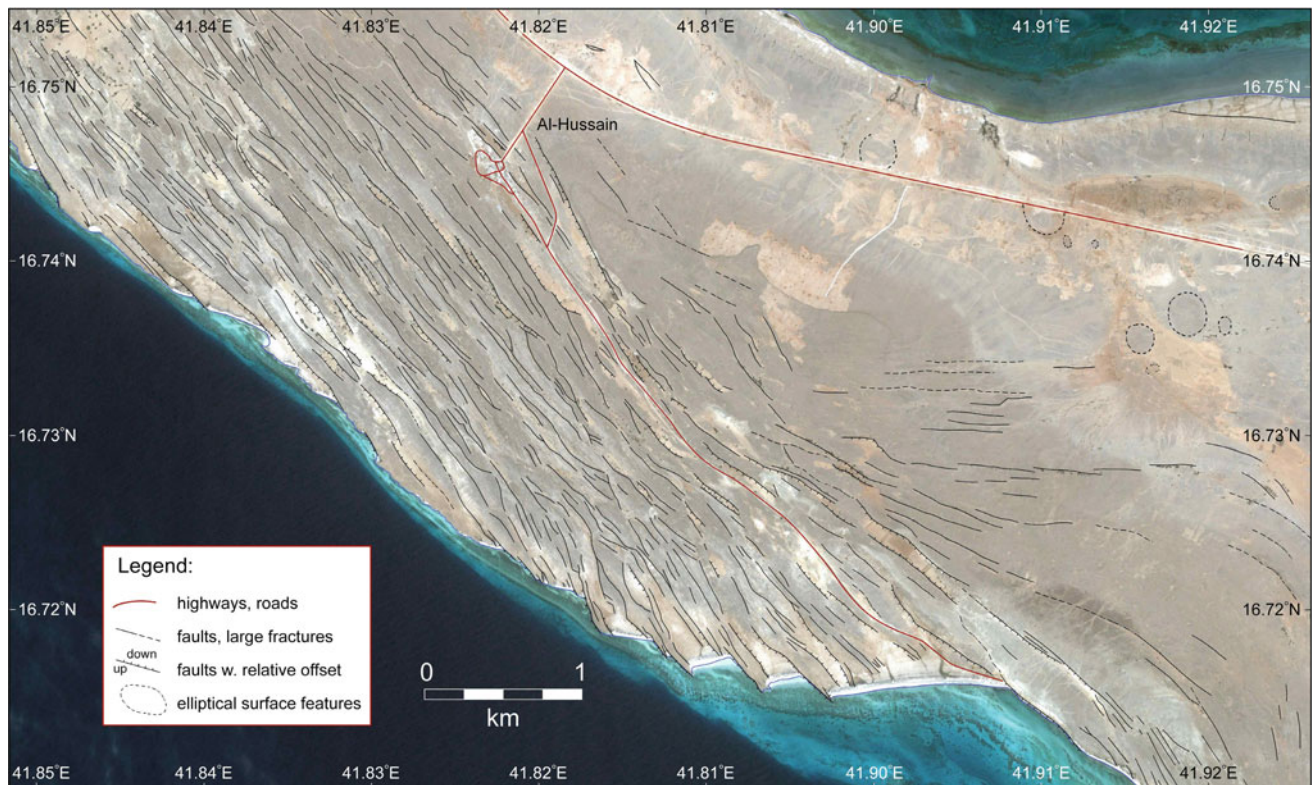


**Fig. 13** Integration of field structural observations and satellite image interpretation for a section of Farasan al Kabir around the village of Al Hussain. Location is shown in Fig. 12. (Google Earth; Image DigitalGlobe 2013)

deposits, perhaps during an interval of minor sea-level regression during an interglacial when the coral and beachrock surfaces were exposed as dry ground suitable for human occupation and activity. The artefacts would, then, represent activity carried out on the nearby bank of the wadi at a time of abundant water supply, close to its confluence with the seashore. This is also consistent with palaeoclimatic data, which indicate that the wettest intervals during long-term palaeoclimatic cycles in the Arabian Peninsula, at least during the late Pleistocene and early Holocene, occurred during the earlier part of interglacials, notably during MIS 5e (Rosenberg et al. 2013). Subsequently the stone artefacts were incorporated into the cobble unit by lateral erosion of the stream bank with minimal disturbance and transportation.

Just what activities were carried out there, apart from stone-tool manufacture, and whether they included the exploitation of molluscs or other marine resources, cannot be known from the evidence currently available. However, the combination of a freshwater stream outlet and a marine shoreline represents a well-known combination of ecological advantages and ecotonal variety generally attractive to plant and animal life and therefore to human settlement, with the addition of marine resources at the shore edge. The ready availability of raw materials for making stone tools from the

local cinder cone, the basaltic lava flows and the cobbles in the stream bed would have offered an added attraction, though this cannot have been the only reason for concentrating activity in this location, given the widespread distribution of these raw materials more widely in the region. Topographic opportunities for trapping large mammals may have been an additional factor (see Kübler et al., this volume). These possibilities reinforce the importance of obtaining dates, and further evaluation must await the outcome of the dating programme.

In the Farasan Islands, the most important observation from an archaeological point of view is the relative rapidity with which shorelines have been elevated because of salt tectonics. This has implications both for where we might expect to find archaeology and coastlines associated with earlier periods of high sea level, and also for the instability of coastal substrates and molluscan habitats on coastlines subject to rapid changes of elevation and geomorphology (see Bailey et al., this volume).

Since the Farasan Islands would have been connected to the mainland during periods of low sea level, there is no reason, in principle, why we should not expect to find MSA or earlier stone artefacts. However, only two surface finds of stone artefacts that might be of MSA type have so far been found on the Farasan Islands, both on the highest elevations



**Fig. 14** Coral terraces and structural features southeast of Al Hussain: **a** ~ 3 m (amsl)-coral platform showing undercutting by marine erosion; **b** ~30-m (amsl) high uplifted terrace, showing marine sediments capped by coral; **c** 120° striking large open fracture cutting

high terrace (width is ~ 60 cm); **d** NW–SE striking small graben on same terrace. Location shown in Fig. 12. Photos: Geoff Bailey (a, b), Bill Bosworth (c, d), November 2014

in the north of Farasan al Kabir, close to the village of Al Hussain (Bailey et al. 2013b). Critical to the evaluation of the potential for habitation in earlier periods of the Pleistocene is the dating of the different coral platforms we have described, and in particular the lowest in the sequence at 2–3 m. This platform, on the shore edge of which many shell mounds are located, forms an extensive land surface in many parts of the Islands, and would have provided important territory for hunting animals and exploitation of other

resources as well as opportunities for marine exploitation at the shore edge. Clearly, when this coral platform was forming underwater, the area of land available for terrestrial exploitation would have been much reduced. Age constraints on the dates of formation of these coral terraces will help to evaluate the potentials of the region for human occupation during earlier periods before the establishment of modern sea level and the appearance of the shell mounds at about 7 ka.

**Table 3** Palaeoshoreline features in the Farasan Islands showing locations visited and samples taken for dating. Data are presented in the same form as in Table 2. Note that all shorelines have been affected to some degree by salt tectonics. Approximate elevations are not corrected for mean sea level or converted to estimates of palaeo sea level

Locality Name	GPS	Description	DGPS Station name	Measured Elevation of Upper Surface (m)	Corrected elevations (m amsl)	Palaeo sea level (m amsl)	Margin of uncertainty (m)	Coral samples for U-series dating	Basalt Samples for $^{40}\text{Ar}/^{39}\text{Ar}$ dating	Shells
Farasan Kabir Is. (2014-11-29-7)	N 16.71564° E 41.89341°	Low terrace in central part of island		~ 4 5.93				FA-001, -002, -003	–	FA-004, -006 (Tridacna) F-005 (Spondylus) F-007 (surface shell)
Farasan Kabir Is. 2014-11-29-8	N 16.71945° E 41.89085°	Large bank of small shells on central fault block terrace		~ 13				–	–	FA-008 (surface shells)
Am Murabaah Is. 2014-11-30-1	N 16.73954° E 42.20501°	Shells on top of island coral terrace	Sulayn	~ 8				–	–	FA-012 (surface shells)
Am Murabaah Is. 2014-11-30-2	N 16.73982° E 42.20495°		Sulayn	~ 10				FA-013	–	–
Am Murabaah Is. 2014-11-30-3	N 16.74007° E 42.20469°	Coral terrace face	Sulayn	~ 13				FA-014, -015, -015A (~ 40 cm below 15)	–	–
Al Abalat Is. 2014-11-30-5	N 16.80652° E 42.18283°	Top of main coral terrace	Sulayn	~ 9				FA-016 (several m's lower in terrace face)	–	FA-017 (surface shells)
Farasan Kabir Is. DGPS St. 3 2014-12-01-3	N 16.62941° E 42.08151°	Uppermost of Ras Sheidah multiple terraces	Farasan Station 3	22.95	24.50	25.55	±0.5	FA-018	–	–
Farasan Kabir Is. DGPS St. 3 2014-12-01-4A	N 16.62950° E 42.08172°	Uppermost of Ras Sheidah multiple terraces	Farasan Station 3	19.99	21.54	22.54	±0.5	FA-019	–	–
Farasan Kabir Is. DGPS St. 3 2014-12-01-4B	N 16.63005° E 42.08369°	Uppermost of Ras Sheidah multiple terraces	Farasan Station 3	20.81	22.36	23.36	±0.5	FA-020	–	–
Farasan Kabir Is. DGPS St. 3 2014-12-01-5	N 16.63056° E 42.08177°	Ras Sheidah intermediate terrace w. sinkholes	Farasan Station 3	15.59	17.14	18.14	±0.5	FA-021	–	–
Farasan Kabir Is. DGPS St. 3 2014-12-01-8	N 16.63229° E 42.08458°	Ras Sheidah intermediate terrace	Farasan Station 3	8.52	10.07	11.07	±0.5	FA-022	–	–
Farasan Kabir Is. DGPS St. 3 2014-12-01-9	N 16.63368° E 42.08331°	Ras Sheidah intermediate terrace	Farasan Station 3	9.07	10.62	11.62	±0.5	FA-023A	–	FA-023B (Tridacna)
Farasan Kabir Is. 2014-12-01-11	N 16.64675° E 42.11082°	Wave cut notch below low ~ 3 m terrace.		~ 3			±0.5	–	–	FA-024 (Tridacna from ~ 1 m below terrace top)
Farasan Kabir Is. Power Station 2014-12-01-13	N 16.68409° E 42.10396°	Low coral terrace		~ 3			±0.5	FA-025	–	–



**Fig. 15** Coral platforms near Ras Sheida on Farasan al Kabir and on the island of Am Murabaah: **a** Deeply undercut ~3 m coral platform to the east of Ras Sheida looking north towards Farasan Town (below letter a); to the right in the distance a line of shell mounds is visible as a series of white mounds on the edge of the bay; **b** Tridacna shell (sample

FA023) embedded in section of ~3-m coral platform at modern shore edge before removal; **c** ~8 m elevated coral platform on Am Murabaah; **d** closer view of the Am Murabaah terrace. Photos: Geoff Bailey, 1 December 2014 (a, b); 30 November 2014 (c, d)

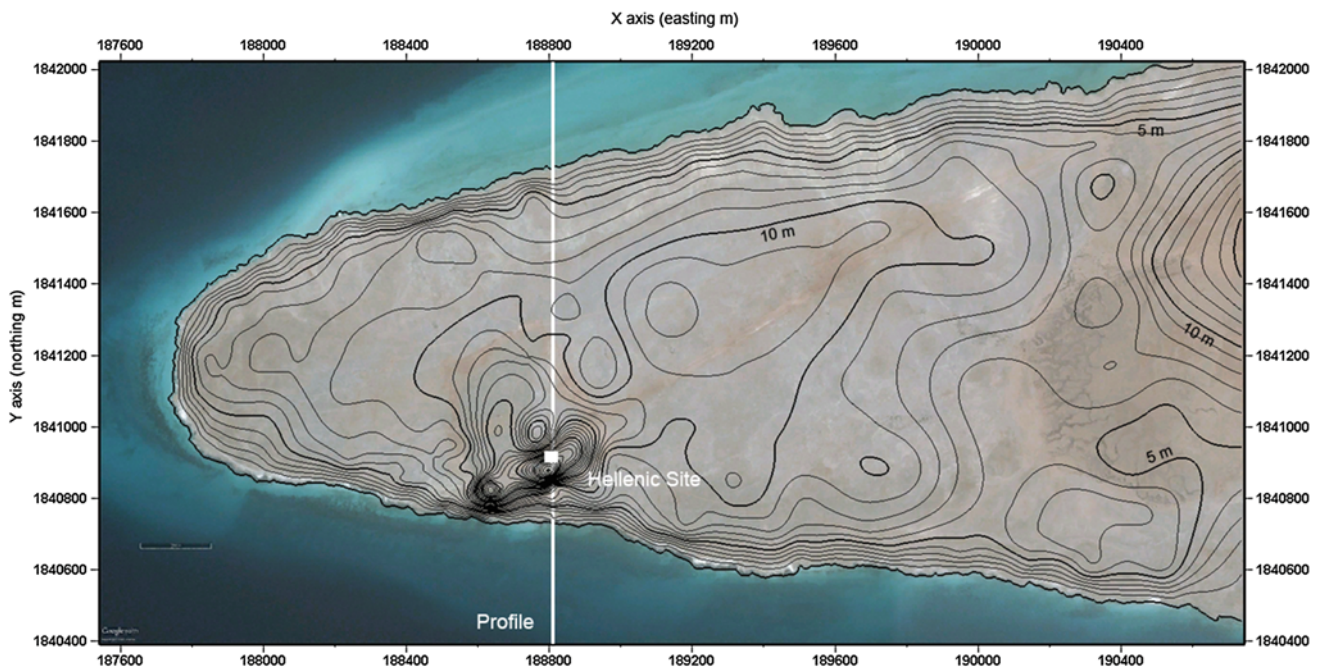


**Fig. 16** Farasan Al Kabir Station 3. Digital elevation model for Ras Sheida peninsula. Contour interval is one metre. Data sources and methodology are described in the text

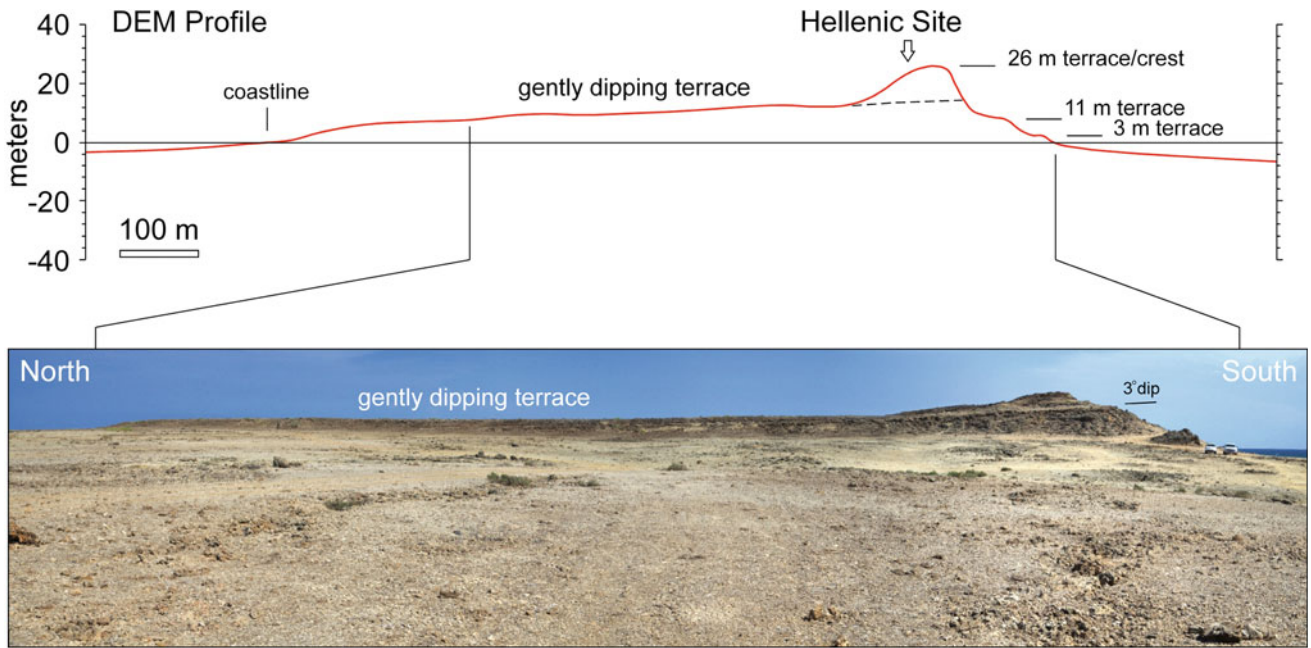


**Fig. 17** Topographic profile across Farasan Station 3 and field view facing east; profile location is shown in Fig. 16. Photo: Bill Bosworth, December 2014

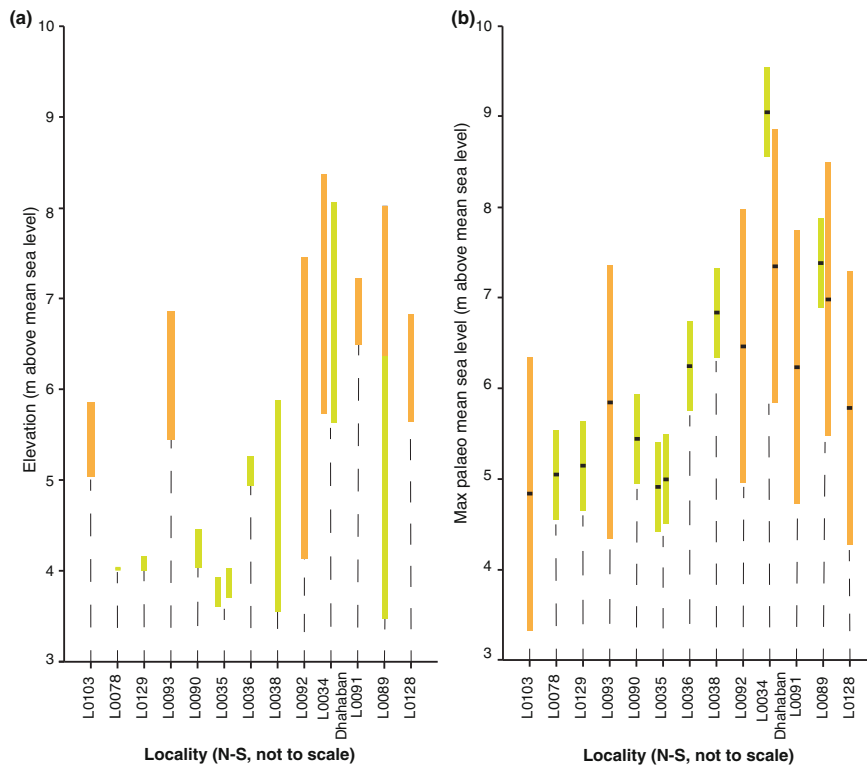


**Fig. 18** Schematic of surveyed marine deposit heights in the Harrat al Birk (a) and the maximum extrapolated palaeo sea level they represent (b). Orange bars for beachrock, green bars for coral. Elevations in (a) were measured from the uppermost extant surface of each terrace or unit (in the case of L0034, L0089), and bars in this graph show the maximum

variability in elevation of the upper surface of the unit across the area surveyed, not unit depth. In (b), the black line represents the maximum elevation of extrapolated palaeo sea level, and the coloured bars the errors associated with this extrapolation

## 9 Conclusion

This work, whilst in its preliminary stages, has recorded and sampled a key archive of fossil marine deposits in the south-eastern Red Sea, deposits that provide benchmarks for relative sea level change and their specific relationship to the archaeological remains left by the populations that inhabited these regions. At least some of the archaeological material we have studied on the coastline of the Harrat al Birk can be stratigraphically linked to an earlier shoreline, and our preliminary investigations indicate that this belongs to MIS 5e at about 125 ka. Our field data are also bringing to light emerging differences of interpretation in relation to the interactions between eustatic changes in sea level, isostatic adjustment and tectonic movements.

Whilst the absence of chronometric dates means that the hypotheses outlined above remain, at present, in need of further testing, it is clear that the emerging data are highlighting new issues in debates about the interactions between sea level change, tectonic movements and the use of coastlines by human populations in the Red Sea during the Pleistocene. Our field data have helped to sharpen the focus on issues in need of further investigation and to identify specific and competing hypotheses and how they can be resolved by chronometric dating. Above all they highlight the ongoing interest and importance of the Red Sea Basin as a ‘laboratory’ for investigating the multiple inter-relationships between sea-level change, tectonic processes, changes in coastal geomorphology and palaeogeography, and the archaeology of early human interest in coastlines and marine resources.

**Acknowledgements** We thank the Saudi Geological Survey for their generous support of this research. We also thank the SCTH for their support of our archaeological research in the region. We also thank two anonymous reviewers for their useful comments. The November–December 2014 fieldwork team comprised Salem Al Nomani, Ali Al Saedi, Fahad Al Rashidi, Thamer Bakaman, Adel Jurais, Mustafa Khorshed, Najeeb Rasul, and Nawaf Widinly (Saudi Geological Survey), Geoff Bailey and Robyn Inglis (University of York, U.K.), and William Bosworth (Apache Egypt Companies, Cairo, Egypt). Bailey and Inglis also acknowledge funding from the European Research Council (ERC) under the Ideas Programme of the 7th Framework Programme as Advanced Grant 269586 ‘DISPERSE: Dynamic Landscapes, Coastal Environments and Human Dispersals’. Inglis also acknowledges funding from the European Union’s Horizon 2020 research and innovation programme under the Marie Skłodowska-Curie grant agreement No. 660343, ‘SURFACE: Human-Landscape-Interactions and Global Dispersals: The Surface Record of Palaeolithic Arabia’. This is DISPERSE contribution no. 40.

## References

- AlSharekh AM, Bailey GN (eds) (2013) Coastal prehistory in southwest Arabia and the Farasan Islands: 2004–2009 field investigations. Series of archaeological refereed studies No. 15. Saudi Commission for Tourism and Antiquities, Riyadh
- Armitage SJ, Jasim SA, Marks AE, Parker AG, Usik VI, Uerpmann HP (2011) The Southern route “Out of Africa”: evidence for an early expansion of modern humans into Arabia. *Science* 331:453–456
- ArRajehi A, McClusky S, Reilinger R, Daoud M, Alchalbi A, Ergintav S, Gomez F, Sholan J, Bou-Rabee F, Ogubazghi G, Haileab B, Fisseha S, Asfaw L, Mahmoud S, Rayan A, Bendik R, Kogan L (2010) Geodetic constraints on present-day motion of the Arabian Plate: Implications for Red Sea and Gulf of Aden rifting. *Tectonics* 29(3)
- Bailey GN (2009) The Red Sea, coastal landscapes, and hominin dispersals. In: Petraglia MD, Rose JI (eds) *The evolution of human populations in Arabia*. Springer, Dordrecht, pp 15–37
- Bailey GN (2015) The evolution of the Red Sea as a human habitat during the Quaternary period. In: Rasul NMA, Stewart ICF (eds) *The Red Sea: The formation, morphology, oceanography and environment of a young ocean basin*. Springer Earth System Sciences, Berlin Heidelberg, pp 595–610
- Bailey GN, Alsharekh AM (eds) (2018) *Palaeolithic Archaeology, Coastal Prehistory and Submerged Landscapes in Southwest Saudi Arabia and the Farasan Islands: DISPERSE field reports, 2012–2015*. Saudi Commission for Tourism and National Heritage, Riyadh
- Bailey G, Carrión JS, Fa DA, Finlayson C, Finlayson G, Rodríguez-Vidal J (2008) The coastal shelf of the Mediterranean and beyond: Corridor and refugium for human populations in the Pleistocene. *Quat Sci Rev* 27(23/24):2095–2099
- Bailey GN, Alsharekh A, Flemming NC, Lambeck K, Momber G, Sinclair A, Vita-Finzi C (2007a) Coastal prehistory in the southern Red Sea basin, underwater archaeology, and the Farasan Islands. In: *Proceedings of the Seminar for Arabian Studies*, vol 37, pp 1–16
- Bailey GN, Flemming NC, King GCP, Lambeck K, Momber G, Moran LJ, Al-Sharekh A, Vita-Finzi C (2007b) Coastlines, submerged landscapes, and human evolution: The Red Sea Basin and the Farasan Islands. *J Island Coast Archaeol* 2(2):127–160
- Bailey GN, Alsharekh A, Flemming NC, Momber G, Moran LJ, Sinclair A, King GCP, Vita Finzi C, Al Ma’Mary A, AlShaikh NY, AlGhamdi S (2012) Coastal archaeology and prehistory in the southwest region of Saudi Arabia and the Farasan Islands: Report on the 2004 and 2006 surveys of the joint Saudi-UK Southern Red Sea Project. *Atlat: J Saudi Arabian Archaeol* 22:134–157
- Bailey GN, Williams MGM, Alsharekh A (2013a) Shell mounds of the Farasan Islands, Saudi Arabia. In: Bailey GN, Hardy K, Camara A (eds) *Shell energy: mollusc shells as coastal resources*. Oxbow, Oxford, pp 241–254
- Bailey GN, Alsharekh AM, Flemming NC, Momber G, Moran LJ, Sinclair A, King GCP, Vita-Finzi C, Al Ma’Mary A, Al Shaikh NY, Al Ghamdi S (2013b) Report on the 2004 and 2006 surveys of the joint Saudi-UK Southern Red Sea Project. In: Alsharekh AM, Bailey GN (eds) *Coastal prehistory in southwest Arabia and the Farasan Islands: 2004–2009 field investigations*. Saudi Commission for Tourism and Antiquities, Riyadh, pp 15–74
- Bailey GN, Devès MH, Inglis RH, Meredith-Williams MG, Momber G, Sakellariou D, Sinclair A, Rousakis G, Al Ghamdi S, Alsharekh A (2015) Blue Arabia: Palaeolithic and underwater survey in SW Saudi Arabia and the role of coasts in Pleistocene dispersals. *Quat Int* 382:42–57
- Bailey GN, Meredith-Williams MW, Alsharekh A (this volume) The archaeology of Pleistocene coastal environments and human dispersals in the Red Sea: Insights from the Farasan Islands
- Bantan RA (1999) *Geology and sedimentary environments of Farasan Bank (Saudi Arabia) southern Red Sea: a combined remote sensing and field study*. PhD Thesis, Royal Holloway, University of London
- Benjamin J, Rovere A, Fontana A, Furlani S, Vacchi M, Inglis RH, Galili E, Antonioli F, Sivan D, Miko S, Mourtzas N, Felja I, Meredith-Williams M, Goodman-Tchernov B, Kolaiti E,

- Anzidei M, Gehrels R (2017) Late Quaternary sea-level changes and early human societies in the central and eastern Mediterranean Basin: an interdisciplinary review. *Quat Int* 449:29–57
- Beyin A (2006) The Bab al Mandab vs the Nile-Levant: an appraisal of the two dispersal routes for early modern humans out of Africa. *Afr Archaeol Rev* 23:5–30
- Bohannon RG (1986) Tectonic configuration of the Western Arabian continental margin, Southern Red Sea. *Tectonics* 5:477–499
- Bohannon RG, Naeser CW, Schmidt DL, Zimmerman RA (1989) The timing of uplift, volcanism, and rifting peripheral to the Red Sea: a case for passive rifting? *J Geophys Res* 94:1683–1701
- Bonatti E, Cipriani A, Lupi L (2015) The Red Sea: Birth of an ocean. In: Rasul NMA, Stewart ICF (eds) *The Red Sea: the formation, morphology, oceanography and environment of a young ocean basin*. Springer Earth System Sciences, Berlin Heidelberg, pp 29–44
- Bosence DWJ, Al-Aawah MH, Davison I, Rosen BR, Vita-Finzi C, Whitaker E (1998) Salt domes and their control on basin margin sedimentation: a case study from the Tihama Plain, Yemen. In: Purser BH, Bosence DWJ (eds) *Sedimentation and tectonics of rift basins: Red Sea-Gulf of Aden*. Chapman and Hall, London, pp 448–464
- Bosworth W (2015) Geological evolution of the Red Sea: historical background, review, and synthesis. In: Rasul NMA, Stewart ICF (eds) *The Red Sea: the formation, morphology, oceanography and environment of a young ocean basin*. Springer Earth System Sciences, Berlin Heidelberg, pp 45–78
- Bosworth W, Stockli DF (2016) Early magmatism in the greater Red Sea rift: timing and significance. *Can J Earth Sci* 53:1–19
- Bosworth W, Taviani M, Rasul N (this volume) Neotectonics of the Red Sea, Gulf of Suez and Gulf of Aqaba
- Bruckner A, Rowlands G, Riegl B, Purkis S, Williams A, Renaud P (2011) *Atlas of Saudi Arabian Red Sea marine habitats*. Khaled bin Sultan Living Oceans Foundation, Panoramic Press, Phoenix, AZ
- Cochran JR (1983) A model for development of the Red Sea. *Bull Am Ass Pet Geol* 67:41–69
- Cochran JR, Karner GD (2007) Constraints on the deformation and rupturing of continental lithosphere of the Red Sea: The transition from rifting to drifting. In: Karner GD, Manatschal G, Pinheiro LM (eds) *Imaging, mapping and modelling continental lithosphere extension and breakup*, vol 282. Geological Society London Special Publications, pp 265–289
- Coleman RG (1993) *Geologic evolution of the Red Sea*. Oxford monographs on geology and geophysics, vol 24. Oxford University Press, Oxford
- Dabbagh A, Emmermann R, Hötzl H, Jado AR, Lippolt HJ, Kollman W, Moser H, Rauert W, Zötl JG (1984) The development of Tihamat Asir during the Quaternary. In: Jado AR, Zötl JG (eds) *Quaternary period in Saudi Arabia: Sedimentological, hydrogeological, hydrochemical, geomorphological, geochronological and climatological investigations in western Saudi Arabia*, vol 2. Springer, Vienna, pp 150–173
- Devès MH, Inglis RH, Meredith-Williams MG, Al Ghamdi S, Alsharekh A, Bailey G (2013) Palaeolithic survey in southwest Saudi Arabia: methodology and preliminary results. *Adumatu* 27:7–30
- Dullo W-C (1990) Facies, fossil record, and age of Pleistocene reefs from the Red Sea–Saudi Arabia. *Facies* 81:175–192
- Dullo W-C, Montaggioni L (1998) Modern Red Sea coral reefs: a review of morphologies and zonation. In: Purser BH, Bosence DWJ (eds) *Sedimentation and tectonics of rift basins: Red Sea-Gulf of Aden*. Chapman and Hall, London, pp 583–594
- El Moursi M, Hoang CT, El Fayoumy IF, Hegab O, Faure H (1994) Pleistocene evolution of the Red Sea coastal plain, Egypt: Evidence from Uranium-series dating of emerged reef terraces. *Quat Sci Rev* 13:345–359
- Erlandson JM (2001) The archaeology of aquatic adaptations: Paradigms for a new millennium. *J Archaeol Res* 9:287–350
- Erlandson JM, Braje TJ (2015) Coasting out of Africa: the potential of mangrove forests and marine habitats to facilitate human coastal expansion via the Southern Dispersal Route. *Quat Int* 382:31–41
- Faure H, Hoang CT, Lalou C (1980) Datations  $^{230}\text{Th}/^{234}\text{U}$  de calcaires corallines et mouvements verticaux à Djibouti. *Bull Societé Géologique de France* 22:959–962
- Girdler RW, Styles P (1974) Two-stage Red Sea floor spreading. *Nature* 247:7–11
- Girdler RW, Whitmarsh RB (1974) Miocene evaporites in Red Sea cores, their relevance to the problem of the width and age of oceanic crust beneath the Red Sea. In: Whitmarsh RB, Weser OE, Ross DA et al (eds) *Initial reports of the deep sea drilling project*, vol 23. Government Printing Office, Washington, pp 913–921
- Groucutt HS, Petraglia MD, Bailey GN, Scerri EM, Parton A, Clark-Balzan L, Jennings RP, Lewis L, Blinkhorn J, Drake NA, Breeze PS, Inglis RH, Devès MH, Meredith-Williams MG, Boivin N, Thomas MG, Scally A (2015) Rethinking the dispersal of *Homo sapiens* out of Africa. *Evol Anth* 24:149–164
- Gvirtzman G (1994) Fluctuations of sea level during the past 400,000 years: The record of Sinai, Egypt (northern Red Sea). *Coral Reefs* 13:203–214
- Hausmann N, Meredith-Williams MG (2017) Seasonal patterns of coastal exploitation on the Farasan Islands, Saudi Arabia. *J Island Coast Archaeol* 12(3):360–379
- Hausmann N, Kokkinaki O, Leng MJ (this volume) Red Sea palaeoclimate: Stable isotope and element-ratio analysis of marine molluscs
- Hendy E, Tomiak P, Collins MJ, Hellstrom J, Tudhope A, Lough J, Penkman KEH (2012) Assessing amino acid racemization variability in coral intra-crystalline protein for geochronological applications. *Geochim Cosmochim Acta* 86:338–353
- Hoang CT, Taviani M (1991) Stratigraphic and tectonic implications of Uranium-series-dated coral reefs from uplifted Red Sea Islands. *Quat Res* 35:264–273
- Hoang CT, Dalongeville R, Sanlaville P (1996) Stratigraphy, tectonics and palaeoclimatic implications of uranium-series-dated coral reefs from the Sudanese coast of the Red Sea. *Quat Int* 31:47–51
- Hubert-Ferrari A, King GCP, Manighetti I, Armijo R, Meyer B, Tapponnier P (2003) Long-term elasticity in the continental lithosphere: modelling the Aden Ridge propagation and the Anatolian extrusion process. *Geophys J Int* 153:111–132
- Inglis RH, Sinclair AGM, Shuttleworth A, Alsharekh AM, Al Ghamdi S (2013) Preliminary report on 2013 fieldwork in southwest Saudi Arabia by the DISPERSE Project: (2) Jizan and Asir Provinces, February–March 2013. <http://eprints.whiterose.ac.uk/80964/>
- Inglis RH, Sinclair A, Shuttleworth A, Alsharekh A, Al Ghamdi A, Devès M, Meredith-Williams M, Bailey GN (2014a) Investigating the Palaeolithic landscapes and archaeology of the Jizan and Asir regions, southwest Saudi Arabia. In: *Proceedings of the Seminar for Arabian Studies*, vol 44, pp 193–212
- Inglis RH, Sinclair AGM, Shuttleworth A, Meredith-Williams MG, Hausmann N, Budd W, Alsharekh A, Al Ghamdi S, Bailey GN (2014b) Preliminary report on 2014 fieldwork in southwest Saudi Arabia by the DISPERSE Project: (1) Jizan and Asir Provinces. <http://eprints.whiterose.ac.uk/80965/>
- Inglis RH, Foulds F, Shuttleworth A, Alsharekh AM, Al Ghamdi S, Sinclair AG, Bailey GN (2015) The Palaeolithic occupation of the Harrat Al Birk: Preliminary report on the 2015 fieldwork in Asir Province, southwest Saudi Arabia. <http://eprints.whiterose.ac.uk/84382/>

- Jerardino A (2017) On the origins and significance of Pleistocene coastal resource use in southern Africa with particular reference to shellfish gathering. *J Anthropol Archaeol* 41:213–230
- Kübler S, Devès MH, Bailey GN King GCP (this volume) Tectonic geomorphology and soil edaphics as controls on animal migrations and human dispersal patterns
- Kopp RE, Simons FJ, Mitrovica JX, Maloof AC, Oppenheimer M (2009) Probabilistic assessment of sea level during the last interglacial stage. *Nature* 462:863–868
- Lambeck K, Purcell A, Flemming NC, Vita-Finzi C, Alsharekh AM, Bailey GN (2011) Sea level and shoreline reconstructions for the Red Sea: isostatic and tectonic considerations and implications for hominin migration out of Africa. *Quat Sci Rev* 30:3542–3574
- Macaulay V, Hill C, Achilli A, Rengo C, Clarke D, Meehan W, Blackburn J, Semino O, Scozzari R, Cruciani F, Taha A, Shaari NK, Raja JM, Ismail P, Zainuddin Z, Goodwin W, Bulbeck D, Bandelt HJ, Oppenheimer S, Torroni A, Richards M (2005) Single, rapid coastal settlement of Asia revealed by analysis of complete mitochondrial genomes. *Science* 308:1034–1036
- Macfadyen WA (1930) The geology of the Farasan Islands, Gizan and Kamaran Island, Red Sea. Part 1. General Geology. *Geol Mag* 67:310–315
- Manaa AA, Jones BG, McGregor HV, Zhao J, Price DM (2016) Dating Quaternary raised coral terraces along the Saudi Arabian Red Sea coast. *Mar Geol* 374:59–72
- Mauz B, Vacchi M, Green A, Hoffman G, Cooper A (2015) Beachrock: a tool for reconstructing relative sea level in the far-field. *Mar Geol* 362:1–16
- McGuire AV, Bohannon RG (1989) Timing of mantle upwelling: Evidence for a passive origin for the Red Sea Rift. *J Geophys Res* 94:1677–1682
- McQuarrie N, Stock JM, Verdel C, Wernicke BP (2003) Cenozoic evolution of Neotethys and implications for the causes of plate motions. *Geophys Res Lett* 30:1–4
- Mellars P, Gori KC, Carr M, Soares PA, Richards MB (2013) Genetic and archaeological perspectives on the initial modern human colonization of Southern Asia. *Proc Natl Acad Sci USA* 110(26):10699–10704
- Meredith-Williams MG, Bailey GN, Hausmann N, Al Ghamdi S, Alsharekh AM, Douka K, Beresford C, Larsen B (2013) Preliminary report on 2013 fieldwork in southwest Saudi Arabia by the DISPERSE Project: (1) The Farasan Islands. [http://www.disperse-project.org/sites/disperse-project.org/files/uploads/DISPERSE\\_2013%281%29\\_01\\_Txt%2Bfigs.pdf](http://www.disperse-project.org/sites/disperse-project.org/files/uploads/DISPERSE_2013%281%29_01_Txt%2Bfigs.pdf)
- Meredith-Williams MG, Hausmann N, Inglis R, Bailey GN (2014) 4200 new shell mound sites in the southern Red Sea. In: Fernandes R, Meadows J (eds) Human exploitation of aquatic landscapes. Special Issue, *Internet Archaeol* 37. <https://doi.org/10.11141/ia.37.2>
- Mohriak WU (2015) Rift basins in the Red Sea and Gulf of Aden: Analogies with Southern South Atlantic. In: Post PJ, Coleman JL, Rosen NC, Brown DE, Roberts-Ashby T, Kahn P, Rowan M (eds) Petroleum systems in “Rift” basins. 34th annual GCSSEPM foundation perkins-rosen research conference, December 13–16, 2015, Houston, CD-ROM, pp 789–826
- Parker AG (2009) Pleistocene climate change in Arabia: developing a framework for hominin dispersal over the last 350 ka. In: Petraglia MD, Rose JI (eds) The evolution of human populations in Arabia. Springer, Amsterdam, pp 39–49
- Penkman KEH, Kaufman DS, Maddy D, Collins MJ (2008) Closed-system behaviour of the intra-crystalline fraction of amino acids in mollusc shells. *Quat Geochron* 3(1–2):225
- Petraglia MD, Alsharekh AM, Crassard R, Drake NA, Groucutt H, Parker AG, Roberts RG (2011) Middle Paleolithic occupation on a Marine Isotope Stage 5 lakeshore in the Nefud Desert, Saudi Arabia. *Quat Sci Rev* 30(13–14):1555–1559
- Petraglia MD, Breeze PS, Groucutt HS (this volume) Blue Arabia, green Arabia: examining human colonisation and dispersal models
- Plaziat J-C, Baltzer F, Choukri A, Conchon O, Freytet P, Orszag-Sperber F, Raguideau A, Reyss J-L (1998) Quaternary marine and continental sedimentation in the northern Red Sea and Gulf of Suez (Egyptian coast): Influences of rift tectonics, climatic changes and sea-level fluctuations. In: Purser BH, Bosence DWJ (eds) Sedimentation and tectonics of rift basins: Red Sea-Gulf of Aden. Chapman and Hall, London, pp 537–573
- Plaziat J-C, Reyss J-L, Choukri A, Cazala C (2008) Diagenetic rejuvenation of raised coral reefs and precision of dating. The contribution of the Red Sea reefs to the question of reliability of the Uranium-series datings of middle to late Pleistocene key reef-terraces of the world. *Carnets de Géologie* 4:1–40
- Reilinger R, McClusky S, ArRajehi A (2015) Geodetic constraints on the geodynamic evolution of the Red Sea. In: Rasul NMA, Stewart ICF (eds) The Red Sea: the formation, morphology, oceanography and environment of a young ocean basin. Springer Earth System Sciences, Berlin Heidelberg, pp 135–149
- Rohling EJ, Grant KM, Roberts AP, Larrasoana J-C (2013) Paleoclimate variability in the Mediterranean and Red Sea regions during the last 500,000 years. *Curr Anthr* 54(S8):S183–S201
- Rose JI, Usik VI, Marks AE, Hilbert Y, Galletti HCS, Parton A, Geiling JM, Morley MW, Roberts RG (2011) The Nubian complex of Dhofar, Oman: An African middle stone age industry in Southern Arabia. *PLoS ONE* 6(11):1–22
- Rovere A, Raymo ME, Vacchi M, Lorschied T, Stocchi P, Gomez-Pujol L, Harris DL, Casella E, O’Leary MJ, Hearty PJ (2016) The analysis of Last Interglacial (MIS5e) relative sea-level indicators: Reconstructing sea-level in a warmer world. *Earth-Sci Rev* 159:404–427
- Rosenberg TM, Preusser F, Risberg J, Pliikk A, Kadi KA, Matter A, Fleitmann D (2013) Middle and Late Pleistocene humid periods recorded in palaeolake deposits of the Nafud desert, Saudi Arabia. *Quat Sci Rev* 70:109–123
- Sakellariou D, Rousakis G, Panagiotopoulos I, Morfisi I, Bailey G (this volume) Geological structure and Late Quaternary geomorphological evolution of the Farasan Islands continental shelf, South Red Sea, SW Saudi Arabia
- Sanderson D, Kinnaird T (this volume) Optically stimulated luminescence dating as a geochronological tool for late quaternary sediments in the Red Sea region
- Siddall M, Rohling EJ, Almogi-Labin A, Hemleben C, Meischner D, Schmeltzer I, Smeed DA (2003) Sea-level fluctuations during the last glacial cycle. *Nature* 423:853–858
- Sinclair AG, Inglis RH, Shuttleworth A, Foulds FW, Bailey GN, Alsharekh A (this volume) Landscape archaeology, Palaeolithic survey and coastal change along the Southern Red Sea of Saudi Arabia
- Spohner R, Oleman P (1986) Topography, Red Sea Region (1:8,000,000). German Research Foundation, Karlsruhe
- Walter RC, Buffler RT, Bruggemann JJ, Guillaume MMM, Berhe SM, Negassi B, Libsekal Y, Cheng H, Edwards RL, von Gosele R, Neraudeau D, Gagnon M (2000) Early human occupation of the Red Sea coast of Eritrea during the last interglacial. *Nature* 405:65–69
- Zarins J, Murad A, Al-Yaish K (1981) The second preliminary report on the southwestern Province. *Atlat* 5:9–42
- Zarins J, Whalen NM, Ibrahim I, Morad A, Khan M (1980) Comprehensive archaeological survey program: preliminary report on the Central southwestern Provinces survey. *Atlat* 4:9–117